USER COM

Information for users of
METTLER TOLEDO Thermal analysis systems

2/99

Dear customer

Even we are sometimes amazed at the vast number of new and existing application areas of thermal analysis. Thermal analysis can be used with great success to solve problems in quality assurance through to research, and for both simple and complex investigations. Newcomers, however, often have difficulty interpreting the curves. Last month we ran our first workshop dealing specifically with this subject. We received so many inquiries that we have decided to organize this workshop again next year.

Contents

DSC purity determination

10

TA-TIP

DSC purity determination can be looked on as a super melting point determination that is increasingly replacing classical melting point methods. The reason for this is that it yields both more information and more accurate results. Based on our 27 years of experience of automatic purity determination, we would like to discuss the most important factors that affect this method.

Validity of the Van't Hoff equation

DSC purity determination is based on the fact that eutectic impurities lower the melting point of a eutectic system. This effect is described by the Van't Hoff equation:

$$T_f = T_0 - \frac{R\,T_0\,T_{fus}}{\Delta H_f}\,\ln(1 - x_{2.0}\,\frac{1}{F})$$

The simplified equation is:

$$T_f = T_0 - \frac{R\,T_0^2}{\Delta H_f}\,x_{2.0}\,\frac{1}{F}$$

where T_f is the melting temperature (which, during melting, follows the liquidus temperature), T_0 is the melting point of the pure substance, R is the gas constant, ΔH_f is the molar heat of fusion (calculated from the peak area), $x_{2.0}$ is the concentration (mole fraction of impurity to be determined), T_{fus} is the clear melting point of the impure substance, F is the fraction melted, ln is the natural logarithm, A_{part} is the partial area of the DSC peak, A_{tot} is the total area of the peak and c is the linearization factor.
In both cases, the reciprocal of the fraction melted (1/F) is given by the equation:

$$\frac{1}{F} = \frac{A_{tot} + c}{A_{part} + c}$$

Non-eutectic impurities can also affect the melting point, and in the case of mixed crystalls, even cause an increase. Impurities that form a an empty two-component system (mutual insolubility in the liquid phase, e.g. vanilline and iron oxide) have no effect at

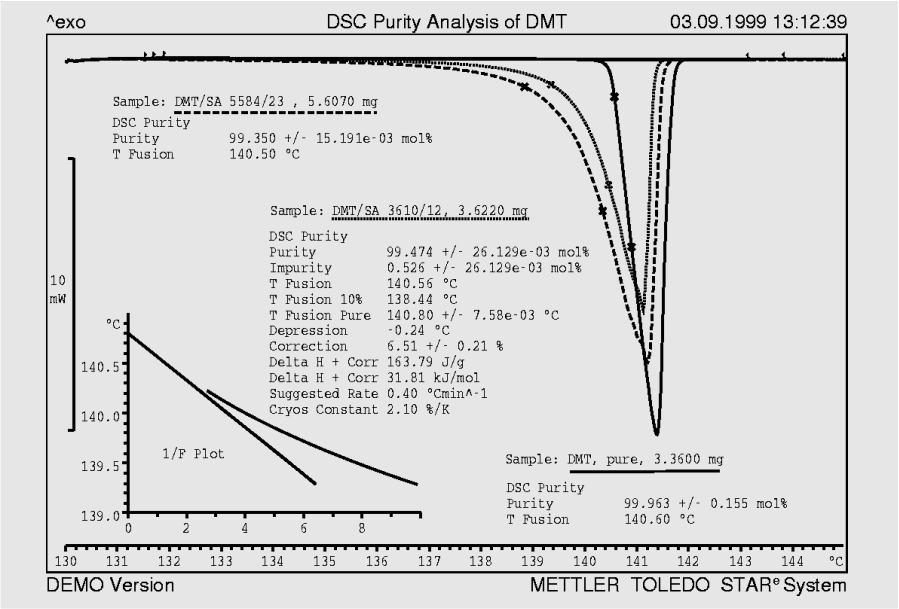

Fig. 1. DSC curves of samples with increasing concentrations of impurity

all on the melting point of the main component. These types of impurity are therefore not detected by DSC purity analysis (except via the lower heat of fusion).

The first thing that has to be checked when validating a method for purity determination is whether the substance under investigation forms a eutectic system with the supposed main impurity. If the chemical process for the production of the substance is known, then usually the by-products are also known; otherwise the chemist must make some intelligent guesses. If necessary, the impurities can often be identified by HPLC. As soon as the main impurity has been identified, samples containing specific amounts of impurity can be prepared and measured by DSC.

This assumes that the main component is available with a degree of purity that is greater than 99.5 mol%. As far as possible, the purity should be checked using different methods and not just by DSC purity analysis alone. The degree of purity can often be improved by recrystallization and zone melting or by drying. Not much substance is needed - 100 mg are usually sufficient for these investigations.

A number of DSC purity determinations are now performed on the main component and the mean value calculated. It is better to prepare samples with increasing concentrations of impurity x_2 directly in the DSC crucible using a microbalance. Samples prepared macroscopically are very often inhomogeneous. If the substances concerned are not already finely powdered, they should be ground and powdered in a mortar and possibly dried in a desiccator.

Weigh several micrograms of the impurity (m_2) into a tared DSC crucible, add several milligrams of the main component (m_1) and note both weights. Seal the crucible immediately and place it in a crucible stand so that its identity cannot be mistaken. In this manner, prepare three to five crucibles with different concentrations of impurity x_2. It is not necessary to mix the components. The intimate contact of the fine powders is sufficient for the eutectic to form by diffusion.

If the molecular masses of the two components are similar, about 10, 20, 50 and 100 micrograms of impurity are used for about 4 mg of the main component. This gives impurity concentrations of about 0.2%, 0.5%, 1% and 2% impurity. To calculate the concentration of impurity in the samples, the molecular masses of the main component (M_1) and of the impurity (M_2) are entered in the following equation:

$x_2 = m_2/M_2 / ((m_1/M_1) + (m_2/M_2))$

The mole fraction is then multiplied by 100% to obtain numbers that are more convenient to use.

DSC purity determinations can now be performed on the artificially contaminated samples using a heating rate of 1 K/min. If the sample melts without decomposition, and recrystallizes on cooling to room temperature, the same sample can be measured again. This improves the shape of the peak at the tip. Any slight decomposition or polymorphism can of course change the shape of the peak.

Try to detect the eutectic peak using the most impure sample. Since the eutectic mixture typically melts some 10 °C to 50 °C lower than the pure component 1, it is a good idea to look for the eutectic peak by measuring a sample that is no longer required at a heating rate of 10 K/min (start temperature about 100 °C below the melting point of component 1). The eutectic peak (Figure 4, left) confirms the presence of a eutectic system.

Plot the error of x_2 (x_2 as determined by DSC minus x_2 added). The ideal case is a horizontal straight line with an error of 0 mol% (Figure 2). If the error is distinctly positive, then dissociation of the impurity is a possible explanation. Sodium chloride in water, for example, gives an "error" of 100% because of the complete dissociation of the Na^+ and Cl^- ions.

m_1 [µg]	m_2 [µg]	Added impurity [mol%]	Measured impurity [mol%]	Error (measured - added) [mol%]
3360	0	0.0	0.037	0.037
3610	12	0.465	0.526	0.061
5584	23	0.58	0.65	0.07
3224	36	1.55	1.45	-0.1
3868	94	3.30	2.77	-0.52

Table 2. Added and measured impurities

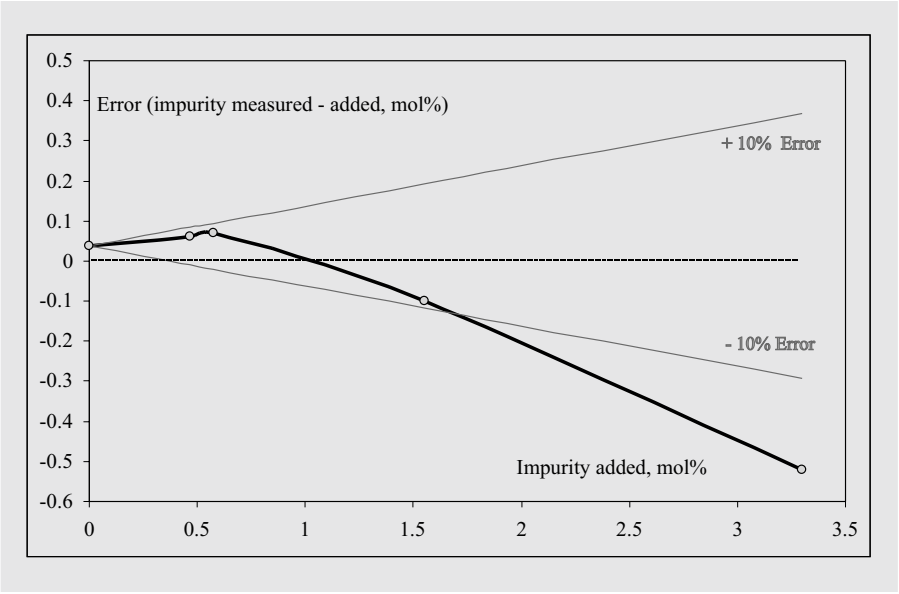

Fig. 2. Error of x_2 as a function of the concentration of added impurity. Component 1 is high purity dimethylterephthalate (M_1 194.2 g/mol), component 2 is salicylic acid (M_2 138.1 g/mol). The sample weights and the results of the DSC purity determination are summarized in Table 1. The error in the DSC purity analysis of this system is less than 10% up to about 1.7% impurity.

Thermal stability of the substance

If the main component undergoes partial decomposition during the melting process, the decomposition products can immediately depress the melting point. This effect decreases noticeably with increasing heating rate because at higher heating rates there is less time for the decomposition to occur.

There are also substances that do not decompose at the beginning of the melting process, but whose baselines after melting are at a different level. In such cases, one makes do with horizontal baselines beginning on the left (low temperature side) of the curve (Figure 4, right).

In principle, the decomposition can be shifted to higher temperature using high pressure DSC at pressures of about 5 MPa. The melting behavior changes very little compared to that at normal pressure.

Volatile impurities

The presence of moisture, i.e. water with its low molecular mass has a large effect on the results of DSC purity determinations. Organic solvents are also examples of volatile compounds that may typically be present. They are included in the evaluation if the measurements are performed in hermetically sealed crucibles.

If only the nonvolatile impurities are of interest, which is normally the case for pharmaceutical active ingredients, then the crucible should be sealed with a pierced lid. Hole diameters of 0.3 mm to 1.0 mm are ideal. The volatile impurities of substances with melting points above about 80 °C can then evaporate and do not affect the results. The endothermic vaporization peak can, of course, give rise to baseline problems which in turn affect the evaluation. This can be avoided by including an isothermal drying period at about 10 °C below the expected melting point. In this case it is important to purge the measuring cell with dry nitrogen (in general, gases from gas bottles are extremely dry).

When using pierced lids, there is of course the danger that not only solvents but also other relatively volatile impurities are lost and thereby not measured.

Small holes (< 0.3 mm) slow down diffusion and result in the formation of a self-generated atmosphere that greatly retards the drying process. If the holes are too large (>1.0 mm) or if crucibles without lids are used, then quite often part of the main component is lost through sublimation.

Polymorphism

Polymorphism interferes with purity determination especially when a polymorphic transition occurs in the middle of a melting peak. With an optimum choice of measurement parameters, the transition can be allowed to take place beforehand in

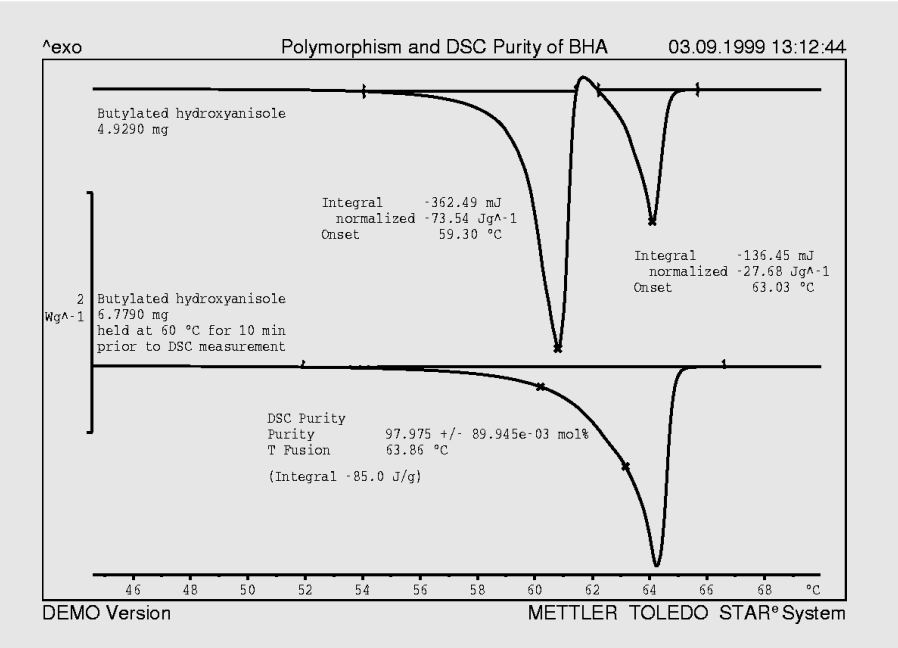

Fig. 3. The upper diagram shows the melting curve of butylhydroxyanisole with the characteristic melting of the metastable modification at about 60 °C, followed by crystallization of the stable modification that finally melts at about 63 °C. Polymorphism interferes with both melting peaks and thereby prevents purity determination. In the lower diagram, the sample is first held at 60 °C for 10 minutes after which the transition to the stable modification is complete. The sample is then cooled down to 35 °C and then heated at 2.5 K/min . Although the melting peak can be evaluated, the results are questionable because BHA contains isomers.

an isothermal segment. Afterwards the resulting stable modification melts in a dynamic segment.
The different modifications of a chemical substance do not mutually depress their respective melting points.
Certain substances exist in partially amorphous form. This manifests itself in a noticeably smaller heat of fusion. A more serious problem for DSC purity determination is exothermic "premelting crystallization" at the beginning of the melting peak, which leads to completely erroneous results. Here again, the crystallization can be allowed to take place isothermally before measuring the melting curve.
With hydrates, (or solvates), two melting points can often be measured. In a hermetically sealed crucible the hydrate melts "in its own water of crystallization", quasi in a eutectic with maximum depression of the melting point. In an open crucible, the water of crystallization evaporates off on warming, and the peak of the resulting anhydrous form occurs at correspondingly higher temperature.

Sample preparation and DSC measurement parameters

Samples: The thermal resistance between the sample and the crucible should be as low as possible. In this respect, fine powders are much more favorable than coarse agglomerates of particles. Furthermore, a sample of fine powder is much more likely to be representative of the substance as a whole.
For these reasons, about 1 g of the substance is ground in a clean agate mortar using as little pressure as possible (the crystal lattice of some substances can be destroyed by excessive pressure). The powder is then stored for future use in a small bottle.
Samples that are liquid at room temperature are prepared by transferring a drop with a fine spatula to a tared standard aluminum crucible. The crucible is then hermetically sealed and weighed. The drop solidifies on cooling in the low temperature DSC.
Sample weight: The heats of fusion of most organic substances are quite large (about 150 J/g), which is the reason why small sample weights can be used. This also reduces the effect of temperature gradients within the sample. A sample weight of 2 mg to 3 mg is optimum for very pure substances, 3 mg to 5 mg for about 2 mol% impurity, and 5 mg to 10 mg for 5 mol% or more impurity. It is good analytical practice to weigh the crucible before and after the measurement in order to check for any losses (this is also advisable for hermetically sealed crucibles since dust or traces of the substance between the crucible and the lid prevent successful cold sealing).
It is often preferable to perform three measurements in order to gain information about the homogeneity of the sample.
Crucibles: The 40 µl standard aluminum crucibles are normally used because they can be hermetically sealed. From the point of view of shape and low heat capacity, the low mass 20 µl aluminum crucibles are also very suitable. They cannot however be hermetically sealed. Sometimes the molten substance is able to seep through the space between the lid and the wall of the crucible (danger of contaminating the DSC sensor).
Start temperature: This depends on the degree of impurity expected and is usually 10 °C to 30 °C below the melting point of the pure substance.
End temperature: This is usually about 5 °C above the melting point of the pure substance.
Heating rate: The optimum heating rate is 0.5 - 1 K/min for very pure substances, 1 -2 K/min for samples with about 2 mol% impurity and 2 - 5 K/min for samples with impurity levels above 5 mol%. A heating rate of 10 K/min can be used for substances that decompose. ASTM E928 lays down heating rates of 0.3 to 0.7 K/min.
Our experience with numerous stable substances shows that the results are not very dependent on heating rates of up to 5 K/min. At 10 K/min, the measured impurity concentration tends to be lower (by about 10%).
If the substance melts without decomposition and crystallizes on cooling, the effect of the heating rate can be investigated by measuring the same sample at different heating rates.
Atmosphere: The DSC cell is usually purged with nitrogen at 50 ml/min in order to prevent oxidative decomposition and to remove any volatile comonents that are formed.

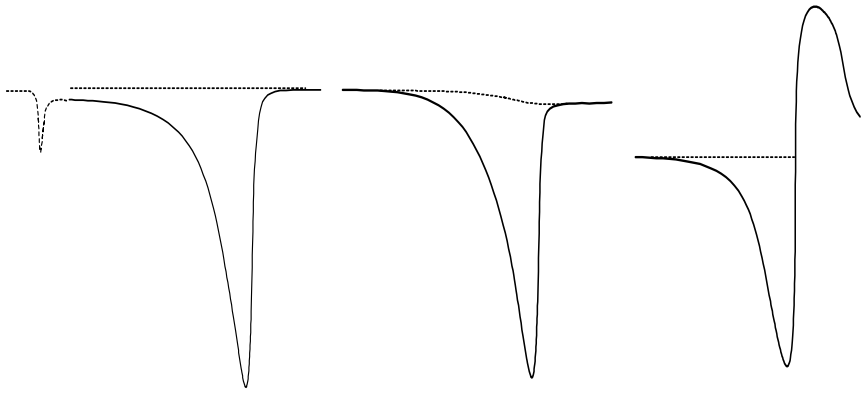

Fig. 4. Schematic DSC melting curves (^exo) with suggested baselines. Left: since the eutectic is usually not measured, the horizontal baseline from the right is a good approximation. Middle: because of anomalous c_p effects, the right side of the baseline can for example be shifted in the endothermic direction. In this case use the Integral or possibly the Spline baselines. Right: the horizontal line from the left is better for substances with marked decomposition after melting.

Choice of the baseline

A horizontal line drawn from the right (after complete melting) is often preferred to the usual line connecting both sides of the peak. This is theoretically the correct baseline since after the eutectic peak small quantities of the pure substance continuously melt. When slight decomposition occurs or with anomalous c_p effects, it is better to use one of the integral baselines, and with more extensive decomposition to use the horizontal line from the left. You will often observe that the linearization correction and to some extent the three confidence intervals are smallest when the baseline is "right".

Tips for the evaluation

The evaluation itself is performed in a selected part of the melting curve, usually in the range 10% and 50% of the peak height. The lower limits exclude excessively high concentrations of impurity in the liquid phase at the beginning of melting. The upper limit eliminates data measured far away from equilibrium conditions. In principle, you can change the limits, for example in order to avoid including an artifact. Another definition of the limits uses peak areas between 10% and 50%. This is advantageous if the eutectic peak lies very close to the that of the pure melting substance (the latter peak is of course evaluated).

In any case, you should check that there are no artifacts of any consequence between the crosses (marked x) where the evaluation is performed.

With higher concentrations of impurity, the "Purity Plus" (logarithmic form) evaluation program gives more accurate results. In addition to this, the heat of fusion of the pure main component can be entered (if the value is known accurately) so that any measurement error is excluded.

Finally some comments on individual points: The linearization correction should be between –10% and +15% of the heat of fusion.

The calculated confidence intervals for 95% probability tell you how good the fit is and hence whether the Van't Hoff equation can be applied. The intervals should not be looked on as " error limits" for the results.

Normally the values for confidence intervals are as follows:

- for the purity (and the concentration of impurity), 0.01 to 0.2 mol%, whereby very pure substances often give relatively "poor" confidence intervals,
- for the extrapolated pure melting peak, 0.005 °C to 0.1 °C and
- for the linearization correction, 0.02% to 5%.

Literature

Futher information and the results of interlaboratory tests can be found in the publication "Purity Determinations by Thermal Methods" (R. L. Blaine, C. K. Schoff, eds.) ASTM-PCN 04-838000-40 ASTM STP 838 (1984).

TGA-FTIR Interface

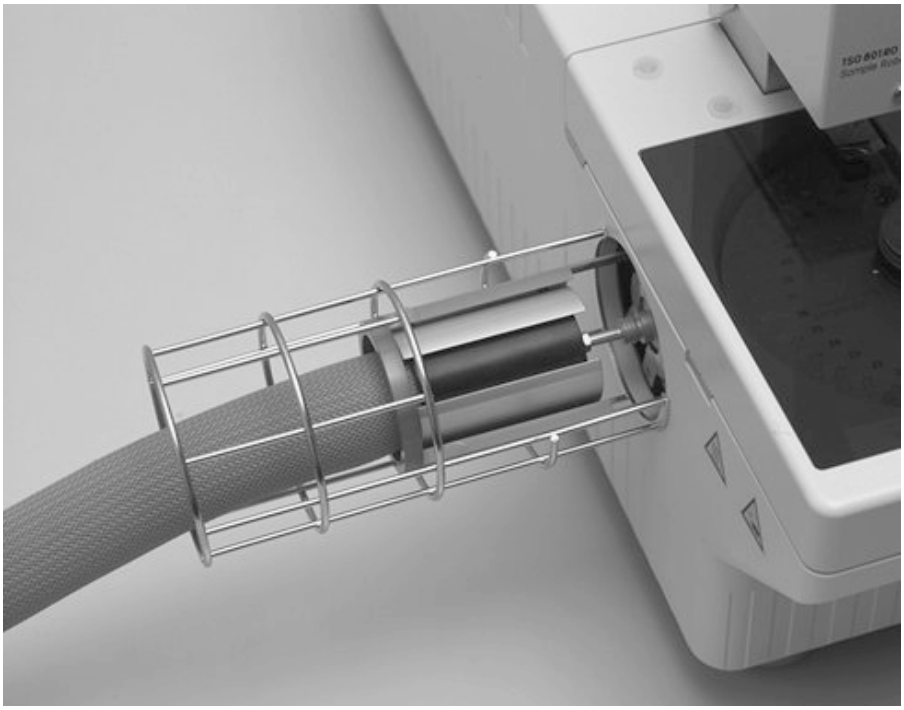

With the new TGA-FTIR interface, Fourier transform infrared spectrometers can be easily interfaced to the TGA/SDTA851^e/LF. A TGA-FTIR system consists of the following components:

Product	Supplier	Order No.
SDTA851^e (large furnace) 1100 °C or TGA/SDTA851^e (large furnace) 1600 °C	METTLER TOLEDO	-
TGA-FTIR Interface	METTLER TOLEDO	51 140 805
FTIR (e.g. Nexus)	Nicolet	-
Gas cell with heated transfer line	Nicolet	-

The Mettler-Toledo TGA-FTIR Interface allows transfer lines with an outside diameter (including insulation) of 25.0 mm to 45.0 mm and an internal diameter of 3.0 mm to be attached.

With the TGA-FTIR combination, you can analyze the decomposition products of TGA samples. Just as with the TGA-MS combination, it provides you with a wealth of new information and makes a meaningful interpretation of the results possible.

TGA-FTIR combination for the investigation of sealing rings

Dr. Frank P. Hoffmann; METTLER TOLEDO GmbH, Giessen

Thermogravimetric Analysis (TGA) is a well-established method that is used in quality assurance and quality control for the characterization of the thermal behavior of a very wide range of substances. With TGA alone, however, it is not possible to learn anything about the composition of the volatile substances evolved from a sample. The online combination of a TGA with a Fourier Transform Infrared Spectrometer (FTIR), however, enables both quantitative (TGA) and qualitative (FTIR) analysis to be performed simultaneously. The technique allows the substances evolved to be identified and correlated with the weight-loss steps detected by the TGA.

The TGA-FTIR combination

The METTLER TOLEDO TGA/SDTA851^e measuring module is interfaced to an FTIR spectrometer (Nicolet Analytical Instruments Nexus or Protege 460). The interface consists of a thermostated gas transfer line that connects the TGA to a thermostated gas cell mounted in the spectrometer. The TGA purge gas flushes the gases evolved from the sample through the transfer line into the gas cell. The IR absorption of the gases is measured in the mid-infrared region. Only a small volume of gas is required for the measurement. This guarantees a high spectrometric detection sensitivity and ensures that the TGA and IR signals coincide.

Apart from the entire IR spectrum, characteristic wavenumber regions can also be selected [1,2], and the changes in the spectrum observed as a function of time or temperature. This method allows the gas mixture evolved to be examined selectively for different components. In this way, relative concentration profiles of the individual components (chemigrams) can be obtained.

The TGA/SDTA851^e module allows a large variation of the purge gas flow rate. This enables the performance of the TGA-FTIR combination to be optimized. With an otimum setting of the flow rate, a good compromise between a sufficiently high product concentration and a short residence time of the gases in the cell can be achieved.

Application example: the thermal stability of sealing rings

The task was to investigate the thermal degradation of sealing rings (elastomers) from two different manufacturers both qualitatively and quantitatively, in order to obtain information about the onset temperature of the initial degradation and any further degradation steps, and to identify the volatile components evolved.

The samples were measured in the temperature range 30 °C to 900 °C at a heating rate of 10 K/min with a nitrogen purge gas flow rate of 40 ml/min. The sample weights used were 27.52 mg and 37.41 mg. The gas cell and the transfer line were thermostated at 200 °C.

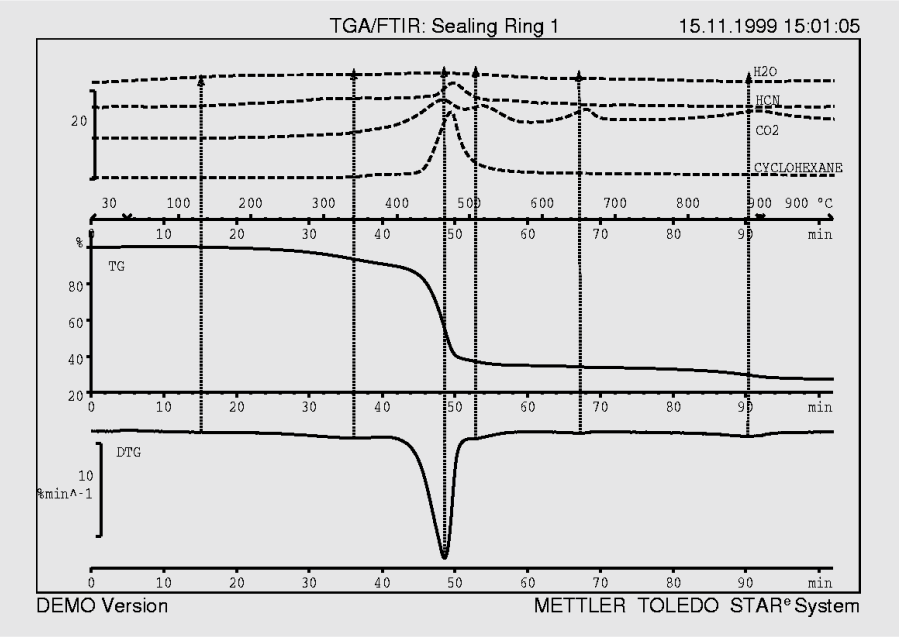

Fig. 1. TGA-FTIR measurement of elastomer sample 1

Figure 1 shows the results for sealing ring 1. In this example, the derivative of the weight loss curve, the DTG curve, was used to identify the individual TG steps. Each step in the TG curve gives rise to a peak in the DTG curve. The TG curve was found to consist of six steps namely at 130 °C, 320 °C, 460 °C, 510 °C, 650 °C and 880 °C. The uppermost diagram shows the chemigrams of H_2O, HCN, CO_2 and cyclohexane. The very small loss of weight at about 130 °C is due to the evaporation of water (0.06%). Afterwards, the decomposition of the nitrile groups leads to the elimination of HCN (0.6%). At the largest decomposition step (53% at 460 °C) HCN, CO_2 and above all cyclohexane are liberated. The latter is formed as a cracking product of the thermal degradation of the polymer chain. The elimination of CO_2 at 650 °C and 890 °C is a result of the decomposition of the filler components (dolomite).

The curves corresponding to the thermal degradation of sealing ring 2 are shown in Figure 2 (the presentation is analogous that in Figure 1). In this sample, only three significant decomposition steps at 220 °C, 330 °C and 470 °C are observed. Afterwards there is a continuous but very gradual loss of weight (1.2%). The chemigram of CS_2 is shown instead of that of H_2O. The very

weak loss of weight detected in the TGA curve at 220 °C (1.3%) corresponds to the formation of carbon disulfide. This results from the decomposition of sulfur compounds formed during vulkanization. HCN and CO_2 are liberated during the second decomposition step (8.1% at 330 °C). Later on, the liberation of cyclohexane begins at about 390 °C in the third decomposition step (53% at 470 °C).
A comparison of the results of the two sealing rings shows differences with regard to the composition of the elastomer and the fillers. The degradation of the polymer chain at about 480 °C is however almost identical in both samples.
Carbon disulfide does not occur as a decomposition product of sealing ring 1.

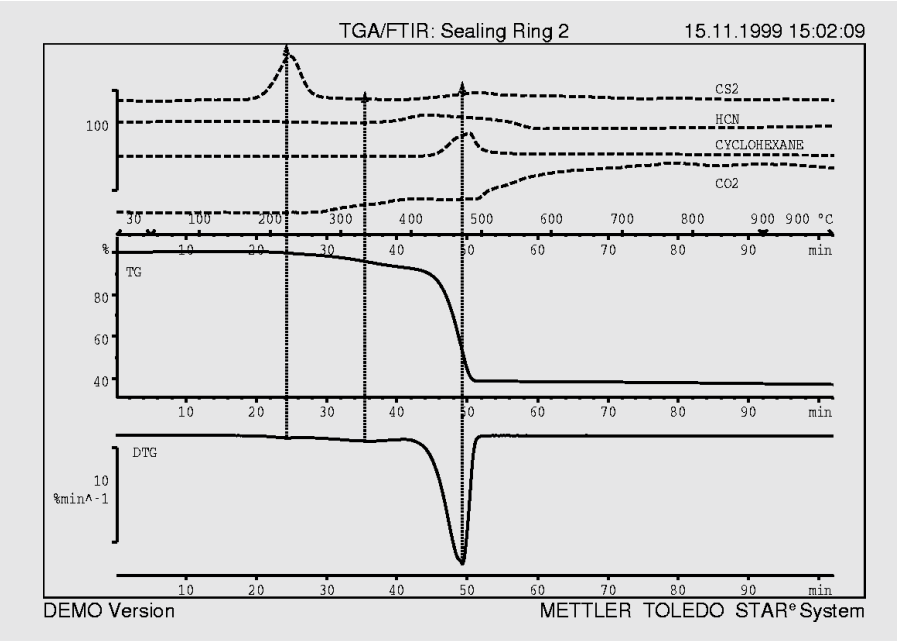

Fig. 2. TGA/FTIR measurement of elastomer sample 2

Summary

The measurements show that a qualitative and quantitative classification with regard to the thermochemical properties of the materials is possible. The combination of TGA and IR spectroscopy facilitates the comparison of materials with given tolerances in quality assurance and in the control of incoming material. The interpretation of the TGA curves is greatly enhanced by the (spectroscopic) separation of the evolved gases into individual components. In addition, this enables a separation of overlapping decomposition reactions to be made, which in turn allows a better insight into the mechanism and kinetics of the decomposition processes.

Literature

[1] Rolf Schönherr: TGA-FTIR Atlas "Elastomers"
[2] Nicolet Vapor Phase Database

Oxidative stability of petroleum oil fractions

Introduction The determination of the oxidative induction temperature is a rapid method for assessing the stability of petroleum oil fractions. The same method can be used to measure the effectiveness of stabilizers. Besides this, aging processes can also be investigated. Standardized isothermal methods are often used instead of dynamic methods (e.g. ASTM D 5483 and ASTM E 1858). Analysis under high pressures of oxygen prevents the vaporization of volatile components and increases the rate of oxidation, thereby shortening the measurement time [1, 2].

Samples Diesel oils of the following petroleum fractions: Light (LGO), Light Cycle (LCGO), Light Vacuum (LVGO), Vacuum1 (VGO1), Vacuum2 (VGO2), Vacuum3 (VGO3) and Kerosine.

Information expected Comparison of the products with respect to their stability in oxygen.

Measurement parameters

Measuring cell	DSC27HP / TC15
Crucible	Aluminum 40 µl, with pierced lid (1 mm hole)
DSC measurement	Put the measuring cell under an atmosphere of oxygen and heat from 40 °C to 150 °C at 20 K/min (to save time), then continue up to 350 °C at 5 K/min. The measurement is automatically terminated when the value of the exothermic DSC signal reaches 10 mW (the combustion peak is not of interest).
Atmosphere	Oxygen at 3 MPa, no purge gas.

Diagram

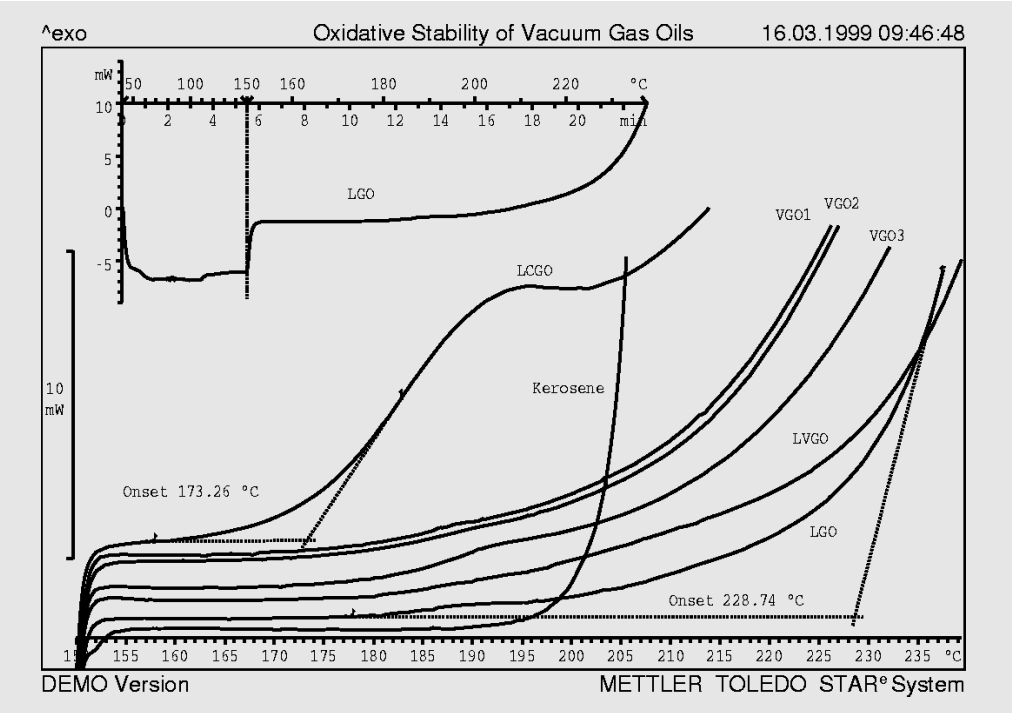

Interpretation

The high pressure of oxygen prevents any premature vaporization so that, on heating, a deflection in the DSC curve is caused only by a change in the specific heat of the sample and no other thermal effects are observed before the beginning of oxidation. The full curve for light diesel oil (LGO) is shown in the upper diagram; the change in the heating rate at 150 °C is marked with a vertical line. The lower diagram shows the measurements of all the samples from 150 °C onwards. The curves are arranged so that they can be seen clearly. The tangents used for the evaluation are drawn for the samples of lowest and highest stability. The abbreviations refer to the petroleum fractions mentioned above.

Evaluation

The oxidative stability is compared by determining the temperature at which oxidation begins (onset). This value is considered to be characteristic of the sample. It is measured as the point of intersection of the horizontal tangent of the baseline before oxidation and the tangent at the steepest part of the DSC curve:

Petroleum Fraction	Abbreviation	Sample weight [mg]	Onset [°C]
Light Cycle	LCGO	4.805	173.3
Kerosine		6.151	203.5
Vacuum	VGO1	6.391	210.4
Vacuum	VGO2	6.016	210.6
Vacuum	VGO3	6.635	214.6
Light Vacuum	LVGO	5.578	224.9
Light	LGO	5.300	228.7

Conclusions

The stability of the various fractions is very different. The DSC curves also show differences at the beginning of oxidation. Similar fractions, however, show almost identical DSC curves with practically the same onset temperatures (e.g. VGO1 and VGO2). This makes it very easy to classify the fractions according to their stability. Long-term stability at low temperatures can, however, only be predicted with kinetic experiments.

Literature

[1] A .T. Riga and G. H. Patterson, Eds., Oxidative Behavior of Materials by Thermoanalytical Techniques, ASTM STP 1326, American Society for Testing and Materials, 1997

[2] H. Kopsch, Thermal Methods in Petroleum Analysis, VCH Verlagsgesellschaft, Weinheim,1995.

What can model free kinetics tell us about reaction mechanisms?

Sergey Vyazovkin, Center for Thermal Analysis, Department of Chemistry, University of Utah 315S. 1400 E., Salt Lake City, UT 84112, USA

Model free kinetics is based on an isoconversional computational technique that calculates the effective activation energy (E) as a function of the conversion (α) of a chemical reaction, $E = f(\alpha)$.
The variation of $E = f(\alpha)$, is not only of importance for reliable predictions, but also allows one to draw important mechanistic conclusions [1, 2]. For instance, the shape of the activation energy curve indicates directly whether a reaction is simple or more complex. For simple processes, $E = f(\alpha)$ is practically constant (horizontal line). Model free kinetics of thermoanalytically measured reactions, however, rarely gives a constant activation energy.
The fact that a reaction is governed by a constant activation energy does not necessarily mean, however, that it is a single step reaction. Most probably it is a multi-step process that is controlled by the rate of the slowest step.
An example of a complex decomposition reaction with almost constant activation energy is the thermal degradation of polypropylene under nitrogen. Figure 1 shows $E = f(\alpha)$ obtained from the model free kinetics of a thermogravimetric study. From the almost constant activation energy of about 180 kJ mol^{-1}, we can conclude that random chain scission is the rate determining step of the degradation reaction.
If $E = f(\alpha)$ is not constant, the process is complex and consists of several reaction steps. Certain complex reactions exhibit a rather typical activation energy dependency $E = f(\alpha)$. For instance, the decomposition reactions of many solid substances are reversible:

$$AB(s) \Leftrightarrow A(s) + B(g)$$

The effective activation energy is given by equation (1), [3]:

$$E = E_2 - \lambda + m\,\Delta H \frac{P_0^m}{P_0^m - P^m} \quad (1)$$

where E_2 is the activation energy of the reverse reaction, λ the heat of absorption, m a constant ($0 < m \leq 1$), ΔH the heat of reaction, P_0 the equilibrium pressure and P the partial pressure of the gaseous reaction product B. From equation 1 it is clear that, as long as the system is not far from equilibrium, the activation energy is temperature dependent because of the temperature dependence of the equilibrium pressure. If, at the starting temperature, the system is virtually at equilibrium (i.e. $P \approx P_0$) then both the last term of equation 1 and the activation energy are large. With increasing temperature, P_0 increases and the system departs from equilibrium, (i.e. $P << P_0$), whereby the last term of equation becomes smaller and decreases to a constant value close to the heat of reaction. The loss of water of crystallization from calcium oxalate monohydrate under non-isothermal conditions is a typical example of this type of kinetic behavior (Figure 2).
If a process involves two (or more) parallel reactions with different activation energies, the contribution of the reaction with the greater activation energy increases with increasing temperature. This is the reason why the experimentally observed activation energy of such processes increases with temperature and therefore also with conversion. An increasing activation energy $E = f(\alpha)$ indicates the occurrence of parallel reactions. An example of this is the kinetics of curing of a DGEBA epoxy resin (diglycidylether of bisphenol A) with phthalic acid anhydride and a tertiary amine as accelerator [4]. The experimentally observed $E = f(\alpha)$ is shown in Figure 3. From this we can conclude that the curing process consists of two parallel reactions with activation energies of about 20 and 70 kJ mol^{-1}. It is known from the literature [5], that curing is initiated by the reaction of the amine with an epoxy group via the formation of a zwitterion. The latter reacts with the anhydride to form a carboxyl anion that catalyses the polyaddition. In a competing reaction, the zwitterion reacts with a hydroxyl group of the DGEBA to form an alkoxide anion which promotes the homopolymerization of the DGEBA. In order to test this hypothesis, we measured the activation energy of the pure competing reaction (DGEBA with the amine but without the anhydride) with DSC. As Figure 3 shows, the polymerization has a practically constant activation energy of about 20 kJ mol^{-1}, which is thus consistent with the value of the competing reaction previously postulated. The low value of E indicates that the process is diffusion controlled. The other reaction with an activation of 70 kJ mol^{-1} is the polyaddition.
Solid phase reactions of the type solid $\rightarrow$ solid + gas often begin under kinetic control and then become more and more diffusion controlled. This is because the thickness of the surface layer already reacted increases, which results in the diffusion of the gaseous product becoming rate determining. The activation energy of the diffusion of a gas in a solid is markedly lower than that for chemical reactions (a few tens of kJ mol^{-1} compared with one to several hundred kJ mol^{-1}). During the transition from a kinetic to a diffusion controlled reaction, one therefore sees a decrease in $E = f(\alpha)$ from about one hundred to several tens of kJ mol^{-1}. This type of dependence is also observed for the pyrolysis of wood [6], (Figure 4).

In summary, it can be said that although the shape of the curve of $E = f(\alpha)$ does not yield any detailled information about the reaction mechanisms, the information is nevertheless adequate for many practical

purposes. If, for example, the rate of a reaction that is initially kinetically controlled and then diffusion controlled is to be increased, then the contribution of slow diffusion must be diminished. This can be done by modifying the starting material (e.g. more finely powdered) and optimizing the reaction conditions.

Literature

[1] S.Vyazovkin, Int. J. Chem. Kinet., 28, 95 (1996).

[2] S.Vyazovkin, C. A. Wight, Annu. Rev. Phys. Chem., 48, 125 (1997).

[3] M. M. Pavlyuchenko, E. A. Prodan, Doklady Akad. Nauk SSSR, 136, 651 (1961).

[4] S. Vyazovkin, N. Sbirrazzuoli, Macromol. Rapid Commun. 20, 387 (1999).

[5] L. Matejka, J. Lovy, S. Pokorhy, K. Bouchal, K. Dusek, J. Polym. Sci. A, 21, 2873. (1983)

[6] S. Vyazovkin, Thermochim. Acta, 223, 201, (1993).

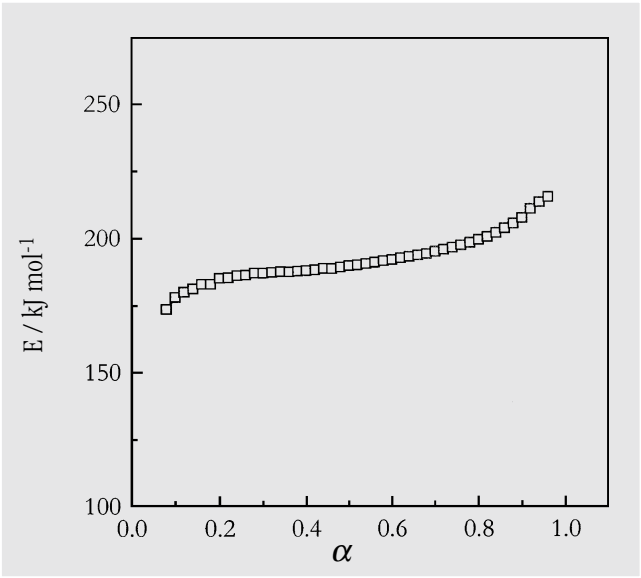

Fig. 1. E = f(α) for the thermal degradation of PP in N_2

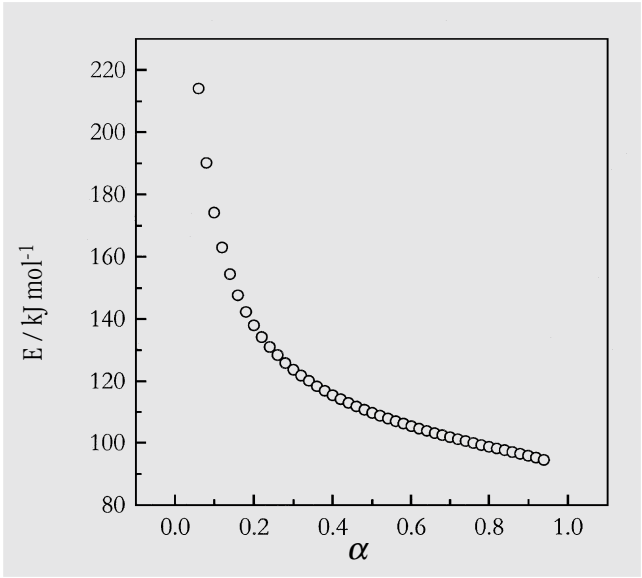

Fig. 2. E = f(α) for the elimination of water of crystallization from calcium oxalate monohydrate in N_2 measured by model free kinetics

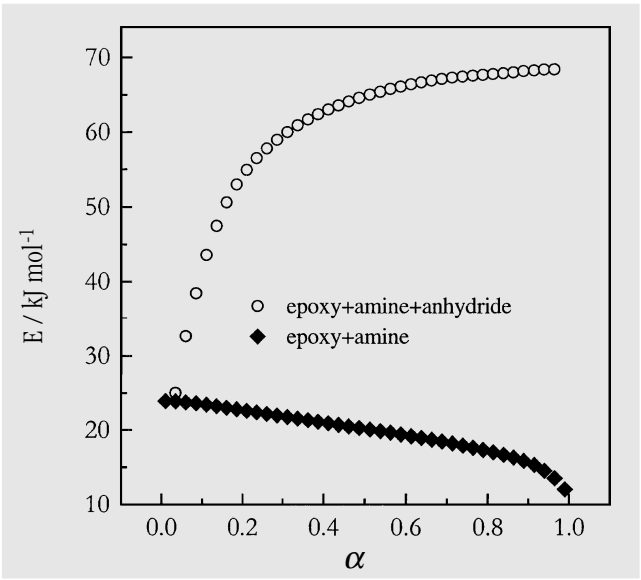

Fig. 3. E = f(α) calculated using model free kinetics with DSC curves. Above: the two parallel reactions of the polyaddition of an epoxy resin yield an activation energy that increases steeply. Below: the isolated homopolymerization reaction at a level of about 20 kJ mol^{-1}

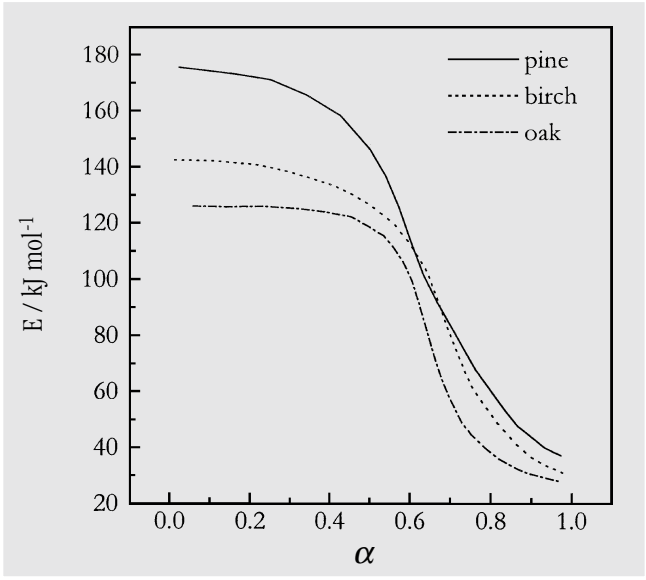

Fig. 4. E = f(α) for the pyrolysis of various types of wood (pine, birch and oak)

Safety investigations with model free kinetics

Scott Barnett, Hexcel Composites, Cambridge, UK

Hexel Composites is a company that manufactures epoxy resin formulations at its production site in Duxford, Cambridge, UK. In order to assure safety in the chemical plant, a thorough understanding of the potential thermal hazards of these materials is essential.
Recently, we started a program to assess the contribution that DSC kinetic data can make. In particular, we wanted to compare the results based on conventional nth order kinetics and the new model free kinetics (MFK) with the data obtained by direct measurement of the adiabatic behavior in hot storage tests (SPS6).

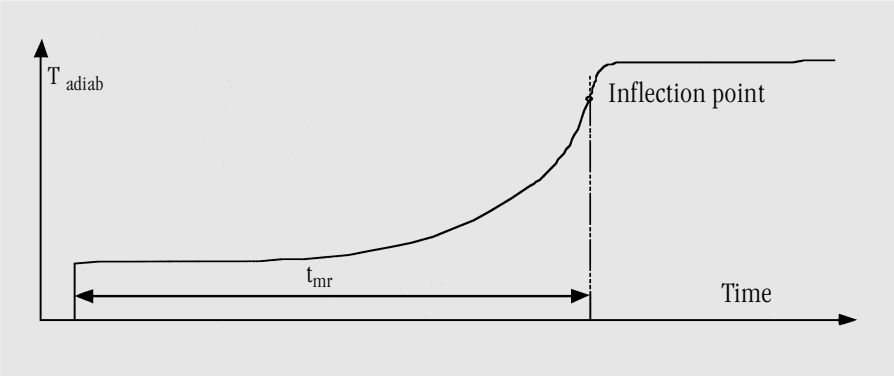

Fig. 1. The measurement begins under adiabatic conditions as soon as the reaction has been heated to the starting temperature T_0. The time taken to reach the maximum reaction rate is known as t_{mr}.

Introduction

Safety investigations frequently assume adiabatic conditions (worst case), in which an initial low level of exothermic energy slowly warms the reaction mass thereby causing the reaction rate to increase until the reaction finally "runs away". The temperature increases by an amount corresponding to the heat of reaction divided by the average specific heat of the reaction mass. At this temperature, organic substances can decompose and give rise to gases and vapors. The time taken to reach the maximum reaction rate (TMR, or as a symbol t_{mr}) is of great importance. This is also sometimes called the intervention time because up until this time an intervention (e.g. cooling) can still successfully prevent an uncontrolled reaction. The TMR can be read off from the curve of the adiabatic temperature increase (point of inflection). The higher the adiabatic starting temperature chosen for the measurement, the shorter the TMR.

Adiabatic hot storage testing is more difficult and expensive to conduct than DSC measurements because it requires both large amounts of sample (up to 1 kg) and specially equipped laboratories to cope ecologically with the fumes that are given off. An alternative to hot storage testing could save much time and expense.

Formulations

Six epoxy resins formulations with amine hardeners were chosen for our investigations. In order to cover a larger temperature range, three formulations with accelerator systems were used (marked with an *), which lower the temperature of cure from 175 °C to 120 °C.

Sample starting	Hardener type number	Usual cure temperature [°C]	Adiabatic temperature [°C]
1	dicyandiamide *	120.0	70.0
2	dicyandiamide	175.0	100.0
3	dicyandiamide *	120.0	60.0
4	3,3'-Diamino-diphenylsulfone	175.0	70.0
5	dicyandiamide *	120.0	62.5
6	dicyandiamide	175.0	70.0

Table 1. Usual cure temperatures and starting temperatures of some types of hardeners

Nth order kinetics

DSC measurements were performed at two different temperatures, namely at the starting temperature of interest T_0 for the calculation of t_{mr} and at a temperature that was 20 °C higher (T_1). (DSC measurements at temperatures below those of the hot storage tests are hardly possible because experimental times are too long and the DSC signals too weak). The activation energy E_a was calculated from these curves using Equation 1.

$$E_a = \frac{R \ \ln(\phi_0 / \phi_1)}{(1/T_0) - (1/T_1)} \quad \text{Equation 1}$$

R is the gas constant 8.314 J mol^{-1} K^{-1} and ϕ is the peak height (in W/g) of the DSC curve at the temperature *T*, the isothermal temperature in degrees Kelvin.
The activation energy could also be calculated directly using the nth order kinetics software option.
The time required to reach the maximum reaction rate under adiabatic conditions, t_{mr}, is then given by Equation 2.

$$t_{mr} = \frac{c_p \ R \ T_0^2}{\phi_0 \ E_a} \quad \text{Equation 2}$$

c_p is the specific heat of the reaction mixture, T_0 the adiabatic starting temperature in degrees K and ϕ_0 the maximum heat output in W/g at T_0.

As can be seen in Table 2, the results obtained from the nth order kinetics do not agree with those from SPS6 measurements. This was in fact expected because the isothermal DSC curves do not take the usual course described by nth order kinetics (the formulations exhibit a delayed increase (formal autocatalysis)) instead of immediately reaching a maximum rate and then steadily decreasing.

Model free kinetics

For these experiments, we performed dynamic DSC measurements at three different heating rates. The model free kinetics software calculates the activation energy as a function of reaction conversion. Model free kinetics allows predictions to be made of the reaction course at almost any temperature (conversion plot). The maximum reaction rate can be read off from each of these conversion curves (most easily from the first derivative). This is multiplied by the heat of reaction (in J/g), in order to obtain ϕ_0 for Equation 2.
The value for t_{mr} from model free kinetics correlates well that from SPS6. This has to do with the fact that model free kinetics can also describe complex reactions with a good degree of accuracy.

Hot storage tests (SPS6)

About 300 g of the freshly prepared formulation were weighed into the Dewar vessel and a thermocouple mounted in the middle of the sample. A graphite block with a hole for the other thermocouple was used as a reference. The Dewar vessel and the graphite reference were placed in an oven at the isothermal temperature of interest T_0. The sample was heated quickly beforehand with a small immersion heater so that it reached the the temperature T_0 in a reasonable period of time. This experimental setup in fact corresponds to a large- scale adiabatic DTA! A pen recorder plots the voltage as a function of time. The time required to reach the maximum reaction rate t_{mr} at the point of inflection of the "DTA curve" is read off from the graph.

Sample number	Adiabatic starting temperature [°C]	t_{mr} from nth order kinetics [h]	t_{mr} from model free kinetics [h]	t_{mr} from SPS6 [h]
1	70.0	0.33	5.7	2.3
2	100.0	2.31	63.0	80.0
3	60.0	1.05	15.2	15.0
4	70.0	2.28	11.3	11.5
5	62.5	0.97	5.2	3.7
6	70.0	2.76	80.0	127.0

Table 2. Summary of the values of t_{mr} obtained by different methods. The results from nth order kinetics are clearly unreliable. The results from MFK are however much nearer the truth.

Conclusions

The time required to reach the maximum reaction rate under adiabatic conditions t_{mr} is an important safety criterion of exothermic chemical reactions.
DSC measurements of the curing reaction of epoxy resin systems can be used to calculate t_{mr} values if they are based on predictions of model free kinetics. Nth order kinetics are not at all suitable for this purpose. For safety reasons, the expensive hot storage tests still cannot be completely eliminated. They are indispensable for new formulations. The effect of small changes in the formulation can, however, be estimated quite well using model free kinetics.

The glass transition from the point of view of DSC measurements; Part 1: basic principles

Introduction

The glass transition is a phenomenon that can in principle occur in all noncrystalline or semicrystalline materials. The requirement is a sufficiently large degree of molecular disorder at least in one direction. To explain the processes that take place during a glass transition we assume for simplicity that we are dealing with a homogeneous liquid.

In a liquid, in addition to the molecular vibrations and rotations (of atoms or groups of atoms) that also occur in solids, there are cooperative movements or rearrangements in which several molecules or segments of molecular chains participate. The cooperative units can be regarded as tempory clusters that fluctuate with regard to both space and time. The size of these cooperative units is typically a few nanometers. This characteristic length decreases with increasing temperature. Another characteristic quantity is the time required for the cooperative rearrangements to take place. It can be described by an internal relaxation time τ.

The glass transition is very sensitive to changes in molecular interactions. Measurement of the glass transition can be used to determine and characterize structural differences between samples or changes in a sample. The glass transition is therefore an important source of information that can be obtained from the thermal analysis of materials. This first article discusses a number of basic principles that aid the interpretation of results. Practical aspects of the glass transition will be dealt with in Part 2 in the next edition of UserCom.

Description of the effect

The thermal glass transition is observed when a melt that is not able to crystallize undergoes supercooling. This phenomenon can be explained by assuming that during cooling, the characteristic time for the cooperative rearrangements approaches the same order of magnitude as the time determined by the measurement conditions (i.e. by the cooling rate). The movements specific to the liquid state "freeze" (vitrification). This results in a reduction of the heat capacity. The temperature at which this effect is observed shifts to lower values with decreasing cooling rate. The glass transition is a dynamic transition of the supercooled melt from a state of metastable equilibrium to a nonequilibrium state (glass).

On heating, the molecular processes "thaw" (devitrification), but at a temperature that is a little higher than that at which they "froze" on cooling. This leads to overheating or enthalpy relaxation peaks in the heating curve.

Figure 1 shows the theoretical change of the enthalpy (the integral of the heat capacity curve) during a thermal glass transition.

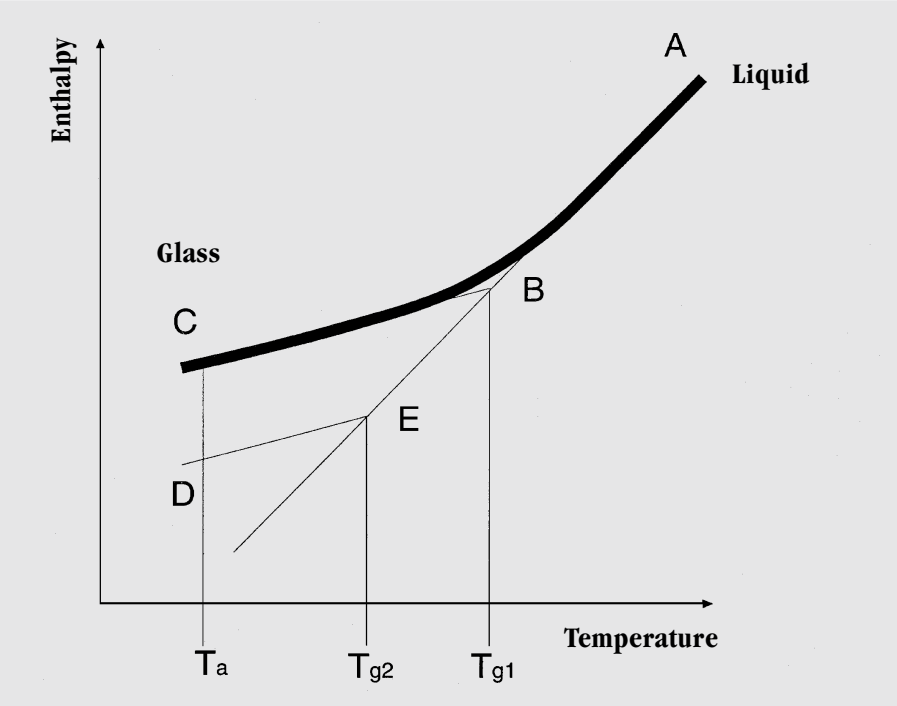

Fig. 1. Theoretical enthalpy curve at the thermal glass transition

The sample is cooled from A to C at a constant rate. Around B it passes through the region of the glass transition with the glass transition temperature T_{g1}. If the sample is then immediately heated up to the point A again, then the same glass transition temperature is measured. Any differences that arise between the glass transition temperature measured in this way on heating or cooling are due to effects of thermal conductivity within the sample. If the sample is held for some time at a temperature T_a, then it ages and the enthalpy becomes smaller. It attains the state designated by the point D. On heating again, the enthalpy intersects the liquid line at the temperature T_{g2} (point E). The glass temperature has changed through aging.

The glass transition temperature T_{g2} can also be attained by cooling from the melt at a lower cooling rate. On cooling, the cooperative units then have more time for their rearrangements to take place, which results in them freezing later. The slower the cooling rate, the lower the glass transition.

As can be seen in Figure 2, hysteresis occurs between the cooling curve and the heating curve even under the same conditions. This effect can be explained by assuming that

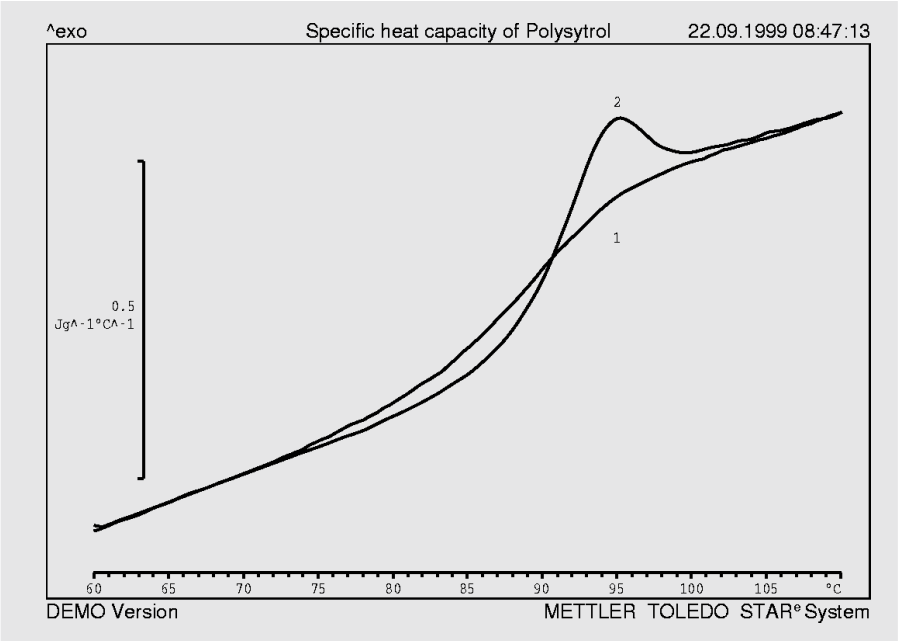

Fig. 2. Specific heat capacity of polystyrene in the region of the glass transition (curve 1 shows the cooling measurement at 2 K/min, curve 2 is the heating measurement immediately after at 2 K/min).

the frozen movements do not thaw until a higher tememperature is reached. Figure 3 shows the differences between the heating and cooling curves in the enthalpy versus temperature diagram. Curve 1 is a cooling curve. No overheating effects occur. The glass transition temperature T_{g1} is the point of intersection of the extrapolated curves of the liquid and the glass. Curve 2 is the corresponding heating curve when the heating and cooling rates are the same. In this curve, relatively small overheating effects occur. The glass transition temperature is T_{g1}. Curve 3 differs from curve 2 only in a more rapid heating rate. This leads to larger overheating effects but the glass transition temperature remains the same. If the heating rate is lower than the cooling rate, the glass transition temperature does not change, but the overheating effect is reduced. Curve 4 represents the measurement of a sample that was heated at the same rate as in curve 2, but which was stored for some time at a temperature T_a below the glass transition temperature. Two effects occur: the glass transition temperature is lower (T_{g2}) and the overheating peak is larger by an amount equal to the value of the enthalpy relaxation ΔH. The process of storage below the glass transition temperature is also known as physical aging.

Figure 4 shows the measurement curves of samples of polyethylene terephthalate (PET) that have been subjected to different periods of physical aging. The shift and the increase in size of the overheating peak can be clearly seen.

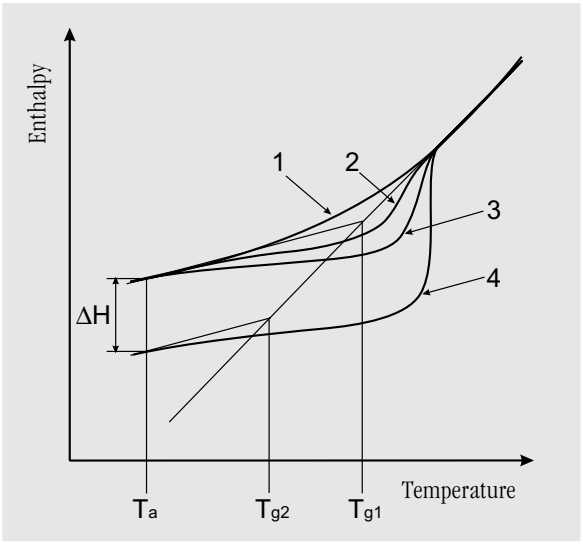

Fig. 3. Theoretical enthalpy curves at the glass transition to illustrate the differences between cooling and heating curves. The curves are described in the text.

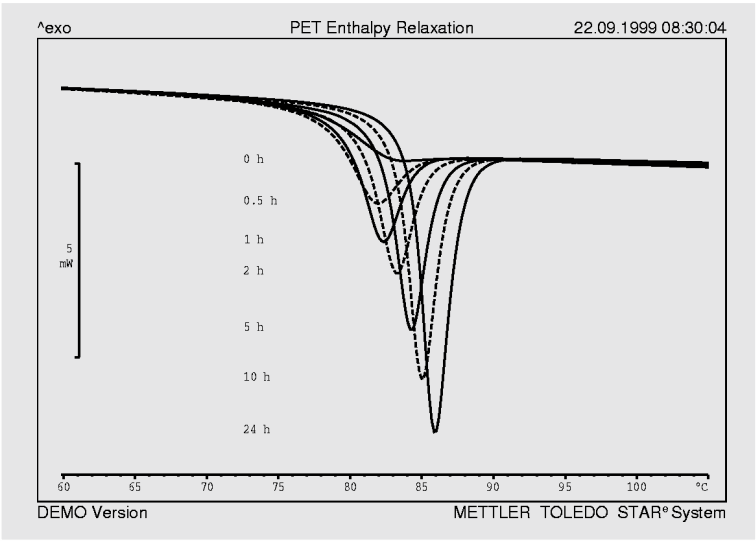

Fig. 4. Heating curves of PET after different periods of physical aging at 65 °C. Heating rate: 10 K/min; Cooling from the melt to room temperature within a few seconds using the sample changer.

Visualization of the glass transition

The glass transition is a kinetic effect that occurs at the transition from a supercooled liquid to a glassy solid state. The processes that occur will be explained with the help of a model.

On cooling a sample that forms a glass, the characteristic relaxation time τ increases with decreasing temperature. This means that the cooperative rearrangements become slower. As can be seen in Figure 5, one can think of the continuous cooling process as being divided up into a series of small steps. At high temperatures (point marked 1 in Figure 5), the relaxation time τ is so short that the sample can completely relax to equilibrium during such a step. The sample is then in equilibrium (liquid). At point 2, the the relaxation time is already appreciably larger. Molecular rearrangements are, however, still rapid enough for the sample to just reach equilibrium during a step. At point 3, the cooperative rearrangements have become so slow that there is not sufficient time for the sample to relax to equilibrium. The molecular rearrangements "freeze". The heat capacity is thereby reduced by an amount corresponding to these rearrangements (c_p step). Only the types of movement specific to solids remain. From this point of view, a glass behaves as a solid although its structure corresponds to that of a liquid.

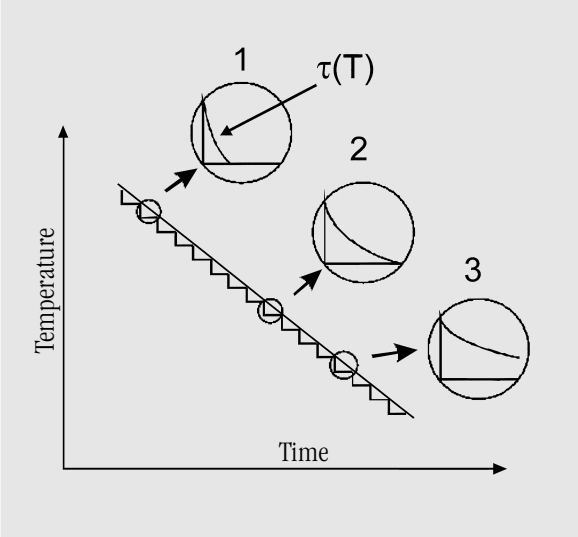

Fig. 5. Illustration of the thermal relaxation with stepwise cooling in the region of the glass transition.

Determination of the glass transition temperature

Various quantities can be used to characterize the glass transition. Besides the glass transition temperature (T_g), the height of the c_p step (Δc_p) and the width of the glass transition (ΔT) are often determined. Other quantities that are used are the height of the overheating peak and its maximum temperature. In Figure 6, a number of characteristic quantities are shown.

Various methods are used to determine the glass transition temperature. Each method gives a somewhat different result, which is why both the evaluation method and the measurement parameters should always be stated. The following is a short summary of the evaluation methods:

- Bisector method: T_g is the temperature at which the bisector of the angle between the two tangents intersects the measurement curve.
- Point of inflection: T_g is the temperature of the point of inflection of the DSC curve.
- Half step height: A straight line extrapolation is performed on the c_p curves of the liquid (c_l) and the glass (c_g). T_g is the temperature at which the measurement curve attains a height equal to half the value of the step height:

$$c_p(T_g) = \frac{c_l(T_g) - c_g(T_g)}{2} + c_g(T_g)$$

- Richardson method: Determination of the fictive temperature of the glass as the glass transition temperature. This temperature corresponds to the intersection of the extrapolated enthalpy curves of the glass and the liquid in the enthalpy temperature diagram shown in Figure 1. In the previous section, only this glass transition temperature was discussed. The determination is done by means of an area calculation (see Figure 7).
  At T_g, $A_1+A_3=A_2$.

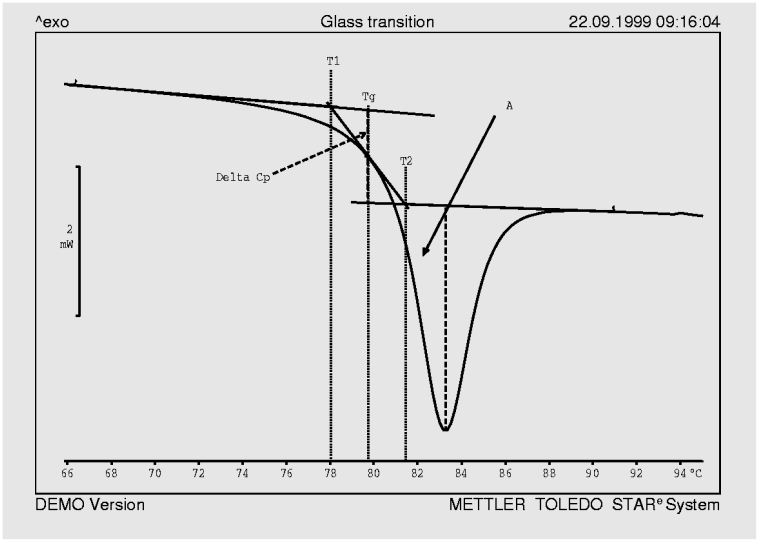

Fig. 6. The figure shows a number of characteristic quantities at the glass transition. T_g: glass transition temperature; ΔT=T2-T2, the width of the glass transition, Delta Cp, the step height ; T_m ,the maximum temperature of the relaxation peak; h, the peak height and A the peak area)

If no overheating peak occurs, the glass temperatures determined by all four methods are almost the same. Larger differences arise between the different glass transition temperatures with curves that exhibit overheating peaks (see Figure 8).

The fictive temperature describes the actual state of the glass. The glass transition temperature determined in this way thereby includes information about the history of the material and its structure. All other methods for determining T_g are not only affected by the state of the glass but also by the actual experimental parameters. They are however useful to identify a sample by its T_g or to evaluate comparative measurements.

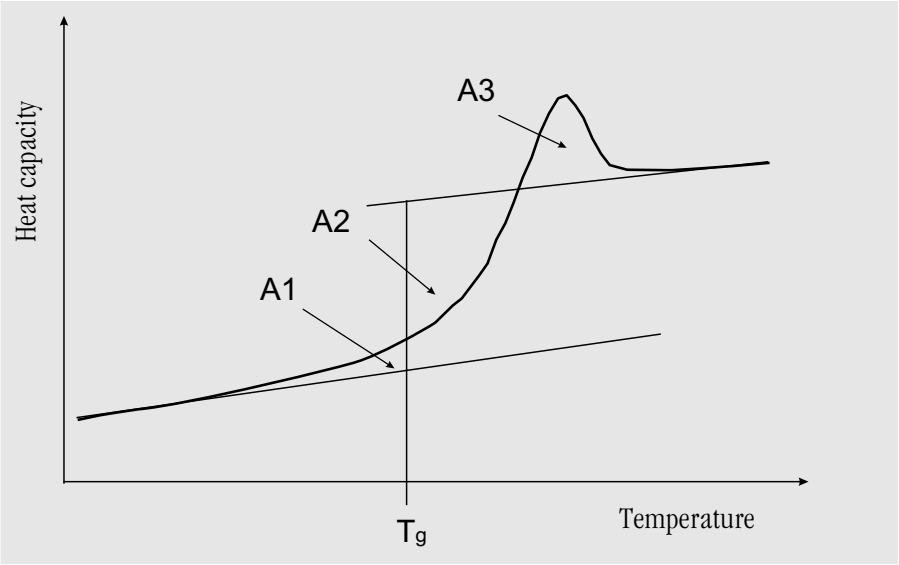

Fig. 7. Determination of the glass transition temperature as a fictive temperature by means of a method based on area caculations.

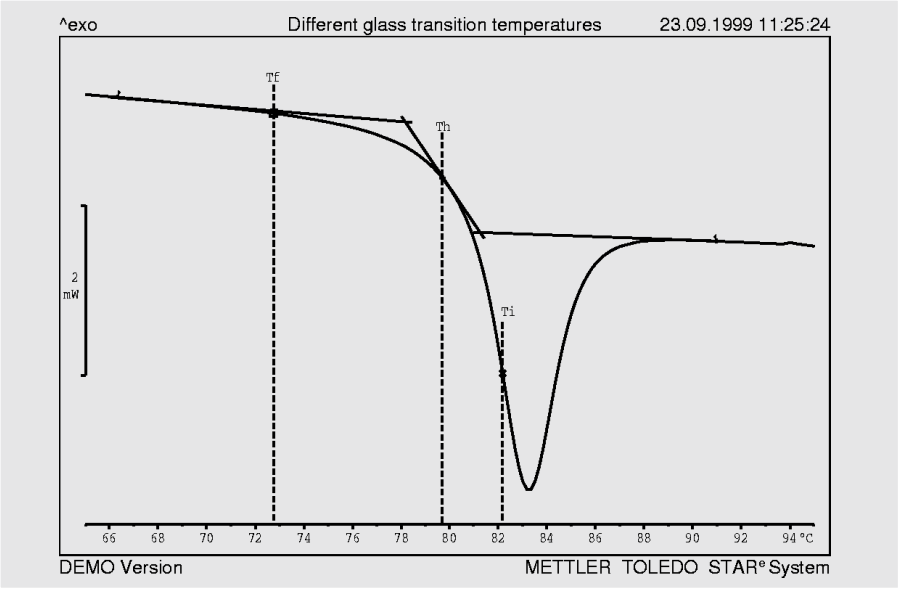

Fig. 8. The figure shows the glass transition temperature determined by different methods (Tf, as the fictive temperature, Th, by the bisector method, Ti, by the point of inflection method).

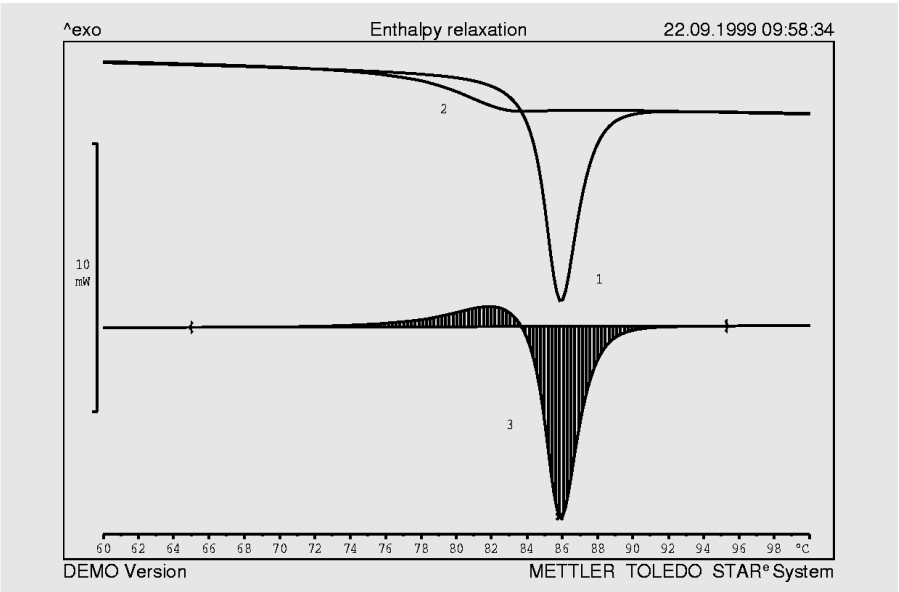

Fig. 9. Determination of the enthalpy relaxation (3.34 J g^{-1}) using a sample that had not been physically aged (second run) using PET as an example (1: first heating run, 2: second heating run of the same sample. 3: difference of the curves of the first and second runs).

Enthalpy relaxation

Enthalpy relaxation in a glass depends on the mechanical and thermal conditions during manufacture and storage. It affects the overheating peak of heating curves.
A method that is frequently used to determine the enthalpy relaxation is to first heat the sample up, then cool it down at the same rate and afterwards immediately heat it a second time. The subtraction of the second heating curve from the first yields the enthalpy relaxation.

$$\Delta H = \int_{T_1}^{T_2} (c_1(T) - c_2(T))\, dT$$

This method is illustrated in Figure 9. A direct determination of the enthalpy relaxation from the area of the overheating peak can lead to large errors.

Determination of the expansion coefficients of an injection molded polyphenylene sulfide machine part above and below the glass transition temperature

Introduction

Parts that are made by the injection molding of fiberglass reinforced polymers usually have expansion coefficients that are direction dependent. The sample investigated here was a machine component (shaft) made of fiberglass filled polyphenylene sulfide (PPS). For the construction of the machine, it was important to know the the expansion coefficients of the shaft in the axial and radial directions. The information was quickly and easily obtained by TMA measurements.

Sample preparation

Measurements of expansion coefficients are performed using the least possible sample loading. To improve accuracy, it is advantageous to use samples that are thick in the direction of measurement. The upper and lower surfaces of the sample should be flat, smooth and parallel. In this investigation, one sample in the radial direction and two samples in the axial direction were prepared from the shaft. Paticular care was taken to minimize any thermal strains when cutting and polishing the samples. The dimensions of the samples were as follows:

Sample A (axial), diameter 9.3 mm, height 4.9 mm,

Sample B (axial, from the other end of the shaft), diameter 5 mm, height 8.7 mm,

Sample C (radial, same end as sample B), height 6.8 mm, area 5 mm x 5 mm.

Measurement parameters

Module: TMA/SDTA840 with a 3.0 mm ball point probe

Load: 0.02 N. A 0.5 mm thick quartz glass disk was placed between the probe and the sample in order to distribute the load uniformly over the surface of the sample.

Temperature program: 30 °C to 200 °C at 1 K/min

Atmosphere: Air, stationary atmosphere.

Results

Figure 1 shows the results of the dilatation measurements on sample A with and without thermal pretreatment. In the first heating run at 1 K/min, a glass transition can be seen which starts at about 78.3 °C. The effect is rather unclear because of enthalpy relaxation. The second heating run, which was also measured at 1 K/min, shows a much clearer glass transition at 91.2 °C. Figure 2 shows the mean values for the coefficients of expansion and the glass transition temperatures of samples B and C (axial and radial direction of the shaft) measured using the second heating run. The results are summarized in Table 1. It is apparent that the glass transition temperatures for the two directions differ by about 3 °C. In addition, the expansion coefficients in the axial and the radial directions differ by about a factor 2 above the glass transition temperature T_g, and by about 30% below T_g. This shows that the orientation (mentioned at the beginning) that oc-

	Axial direction	Radial direction
Glass transition temperature, T_g	91.1 °C	94.0 °C
Expansion coefficient below T_g	25.1 ppm/K	35.8 ppm/K
Expansion coefficient above T_g	50.5 ppm/K	88.73 ppm/K

Table 1. Glass transition temperatures and the mean coefficients of linear expansion in the axial and radial directions.

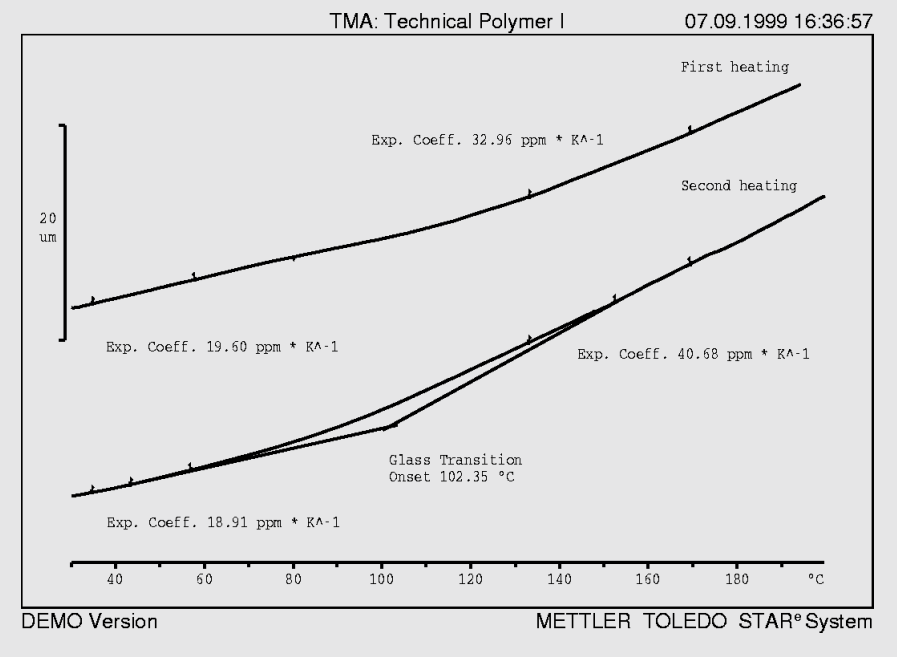

Fig. 1. The first and second TMA heating heating curves of sample A (axial). The mean linear coefficients of expansion have been evaluated.

curs in injection molded parts during the production process has a considerable effect on the mechanically determined glass transition temperature and on the coefficients of thermal expansion.
A comparison of the mean coefficients of expansion of the two samples in the axial direction (sample A and sample B) shows small but neverless significant differences. This indicates that the different flow paths also have an effect on the thermal properties of the injection molded part. In other words, one can detect not only direction dependent anisotropic behavior, but also location dependent effects (which are course appreciably smaller).

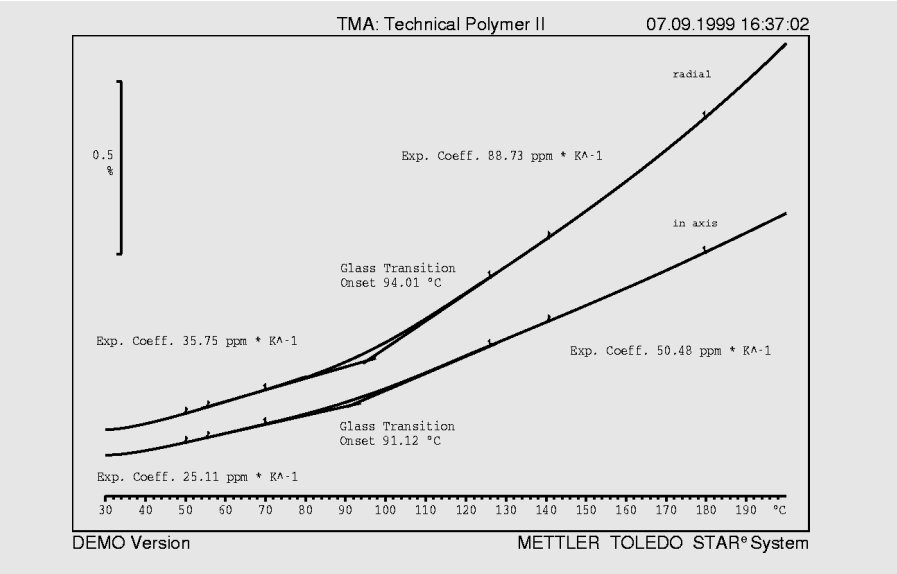

Fig. 2. TMA curves showing the glass transition and the mean coefficients of linear expansion in the axial and radial directions of the PPS injection molded part (samples B and C).

Two-component phase diagram and the determination of the eutectic composition of dimethyl terephthalate (DMT) and benzoic acid

Introduction

The regions in which the various phases of a binary mixture are in equilibrium can be described by a so-called two-component phase diagram in which the temperature is plotted as a function of composition. The term eutectic melting diagram is also used if we are dealing with solid-liquid transitions.
There are in fact 12 different basic types of two-component melting diagrams (see for example [1]). In practice, however, we often encounter euctectic systems whose two-component phase diagrams are of the type shown schematically in Figure 1.

Two-component phase diagrams from DSC measurements

These types of two-component phase diagrams can be determined by DSC measurements. To do this, samples containing mixtures of the two substances in different ratios are prepared and measured by DSC. Points on the liquidus line are determined

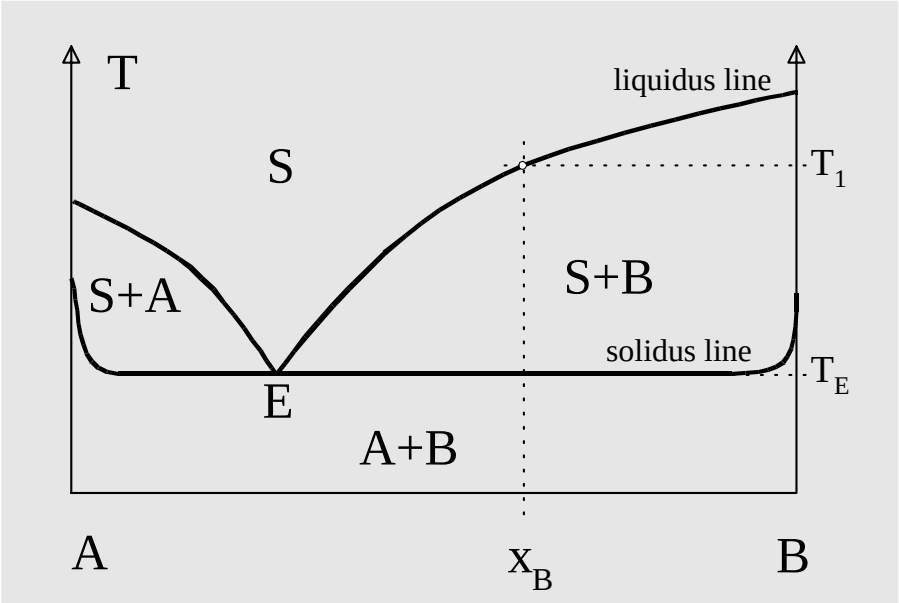

Figure 1: Below the solidus line both substances exist in separate crystalline forms in the solid state. If the temperature of a mixture of the two components is slowly raised, a portion of the sample melts at the melting point of the eutectic. In this liquid mixture phase, either pure A or pure B in the solid state is also present depending on whether one is on the left or the right side of the eutectic composition. On further heating, the remainder of the solid phase melts until finally the whole sample has completely melted at a temperature corresponding to the initial composition of the mixture x_B. Above the liquidus line there is only one phase (homogeneous melt).

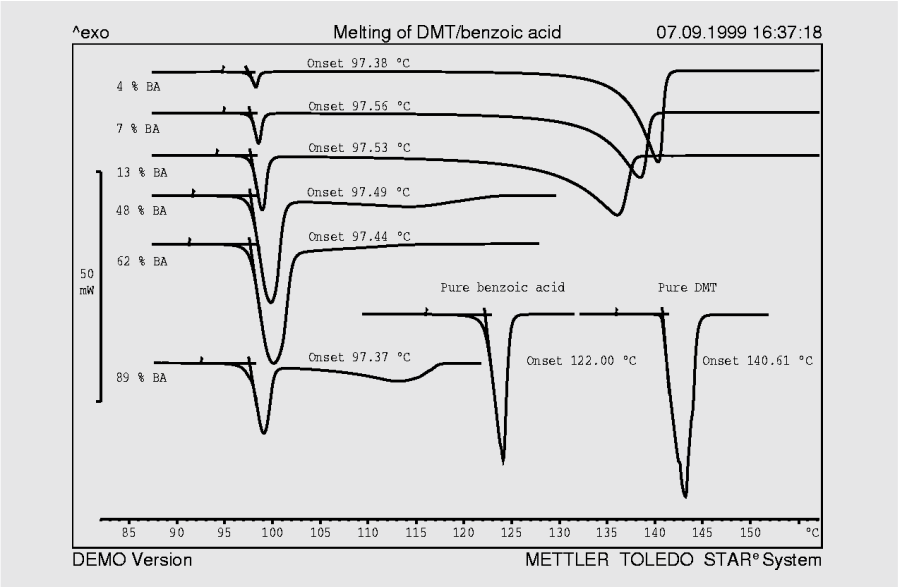

Fig. 2. DSC curves of different mixtures of DMT and benzoic acid. The benzoic acid content is given in units of mole percent.

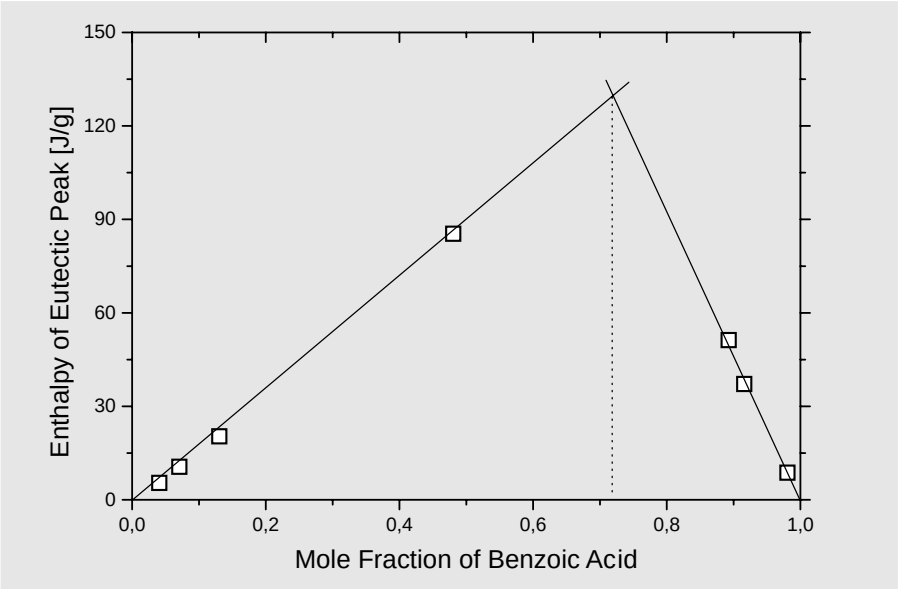

Fig. 3. Determination of the eutectic composition of DMT and benzoic acid.

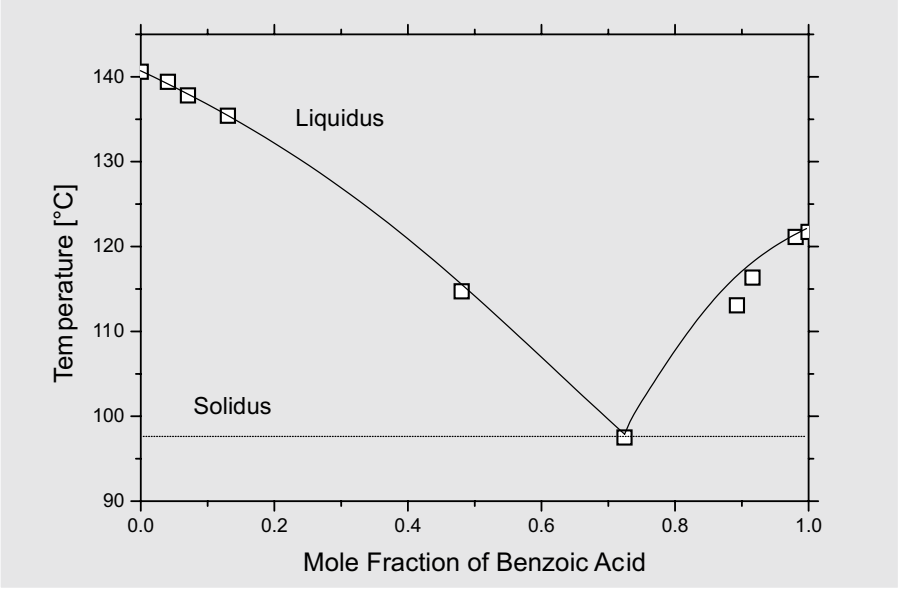

Fig. 4. Two-component phase diagram of DMT and benzoic acid.

by measuring the clear melting points of the different samples and plotting these as a function of the composition of the sample. The clear melting point (the temperature at which melting is complete) corresponds approximately to the temperature of the maximum of the second peak, i.e. the melting peak of the pure (main) component.

These types of measurements can also be used to determine the eutectic composition: the heat of fusion of the eutectic melting peak is plotted against composition and the eutectic composition obtained by extrapolation. This is appreciably more accurate than extrapolating the nonlinear liquidus temperatures. In this way, the melting point of the eutectic (solidus line) and an additional point of the two-component phase diagram have been determined.

Results

This method is illustrated in Figures 2 to 4 using the system dimethyl terephthalate (DMT) and benzoic acid as an example. Figure 2 shows the DSC curves for various mixtures with different ratios of DMT and benzoic acid. As expected, the eutectic always melts at the the same temperature. The heat of fusion of the eutectic peak is however different in each case because of the different sample compositions. The plot of the heats of fusion of the eutectic peaks against sample composition (Fig. 3) yields a value of 72 mol% for the eutectic composition. The two-component phase diagram of DMT and benzoic acid can then be plotted from the melting points of the peaks (see Fig. 4).

Measurement parameters

Module:
DSC821^e, stationary air atmosphere
Temperature program:
70 °C to 160 °C at 5 K/min
Sample weights:
between 4 mg and 8 mg

References

[1] Landolt-Börnstein,
Schmelzgleichgewichte , 6th Edition,
Volume II/ Part 3, page 1

Crosslinking and degree of cure of thermosetting materials by Differential Scanning Calorimetry (DSC)

Dr. Bernhard Benzler; METTLER TOLEDO GmbH, Giessen

Thermosets (or thermosetting plastics) is the term used to describe a group of hard and amorphous plastics that remain rigid up until their degradation temperatures. They consist of close-meshed cross-linked macromolecules and cannot therefore melt or be dissolved.

Phenolics and aminoplastics, epoxy resins (EP resins) and unsaturated polyester resins (UP resins) are examples of thermosetting materials. The former are polycondensation products whereas the latter are made by polyaddition and polymerization. The precursor products are known as thermosetting resins. Following the addition of additives (hardeners, accelerators, fillers, etc.), they react or cure to form thermosets.
In practice, thermosets can be found in very many different forms: with fillers in moldings such as drinking cups, unreacted as powder coatings, and fiberglass reinforced as composites and constructional materials for printed circuit boards in the electronics industry. Typical for these thermosetting materials is that the polymerization normally takes place during the molding process because they cannot be shaped thermoplastically.
The properties of the products depend to a large extent on the degree of the polymerization. As part of a quality assurance program, tests are essential to check the properties of the products for their intended use. A suitable control method should be easy to perform and give a high degree of reproducibility, and the sample preparation should be relatively simple. Spectroscopic methods, for example, cannot normally be used because of the insolubility of the crosslinked product. In practice, two thermoanalytical methods, namely Thermomechanical Analysis (TMA) and in particular Differential Scanning Calorimetry (DSC), have been very successful and have in fact become standard methods.

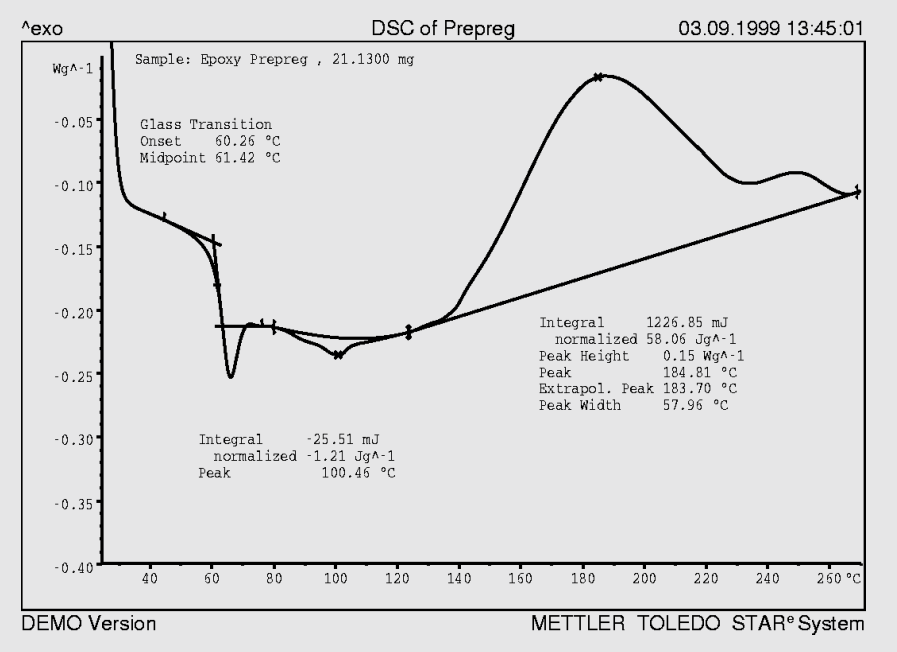

Fig. 1. This shows a typical DSC heating curve (heating rate 10 K/min) of a thermosetting resin , in this case an epoxy resin such as is used for the production of printed circuit boards in the electronics industry.

The measurement curve first shows an endothermic step at about 60 °C due to a glass transition. The resin is transformed from a glassy brittle state to a rubbery state. The glass transition is clearly overlapped by a so-called enthalpy relaxation effect that would no longer be observed if the sample were immediately measured again after cooling. The small endothermic peak with a maximum at about 100 °C is caused by the melting of additives (e.g. catalyst, accelerator, etc).
Under the conditions used for this experiment, the curing reaction begins at about 130 °C and is observed as a large exothermic peak in the temperature range up to about 270 °C. The peak maximum, i.e. the temperature at which the greatest formation of heat or the greatest reaction rate occurs, is at about 185 °C. A second maximum at about 250 °C shows that the reaction consists of different steps. The total heat of reaction is determined by integration. This quantity can serve as a reference value to evaluate the completeness of the reaction, for example when the postcuring reactions of a series of production samples are measured under the same conditions. Such postcuring effects are, however, difficult to detect if the degree of cure is already more than 95%.

The parameters of the glass transition, however, provide a more sensitive measure of the degree of cure, in particular the glass transition temperature T_g and the size of the accompanying change of the specific heat capacity c_p. With increasing

crosslinking, the freedom of movement in the polymer decreases, resulting in a shift of T_g to higher temperature and a decrease in Δc_p.
Distinct differences in the shape of the curves are already clearly visible above about 130 °C - the curve of the postcured sample has the smallest exothermic effect, i.e. the least amount of postcuring.
The glass transition temperature T_g of the finished product is of vital importance for its use because many important properties change at the glass transition (e.g. the modulus of elasticity, the coefficient of thermal expansion and the dielectric loss factor). Neglecting the control of the glass transition can, for example, result in printed circuit boards that are incompletely cured, which in turn results in damage on flow soldering.

The parameters of the glass transition differ greatly:

	T_g [°C]	Δc_p [J/(g K)]
Epoxy resin (first heating run)	66	0.40
after isothermal curing	106	0.29
second heating run	120	0.27

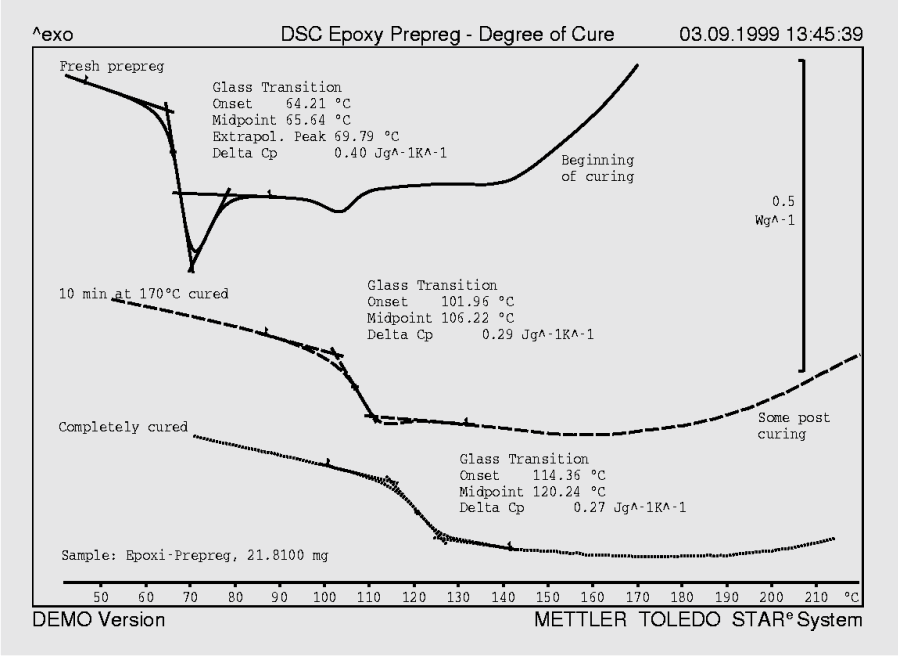

Fig. 2. This shows three DSC heating curves that were measured at a heating rate of 20 K/min. One of the samples is identical to the resin measured in Figure 1, so that the curve obtained (continuous line) is practically the same despite the more rapid heating rate. The second sample was allowed to react by maintaining it isothermally at 170 °C for 10 minutes , cooled and afterwards examined by heating up to 220 °C (dashed line). The third curve (dotted line) is the repeat measurement of this sample. The DSC measurements led to the complete postcuring of the isothermally cured sample.

Conclusions

The examples described show that differential scanning calorimetry (DSC) is able to provide information about the reactivity and the crosslinking or degree of cure of a resin or resin system. The sample preparation is easy and the measurement straightforward and rapid. This is not only true for the epoxy system described above but also for other resin systems. Condensation resins give rise to volatile by-products and should be measured in sealed and pressure-tight crucibles. The same is true if volatile components are present, e.g. solvents.
The measured heat of reaction is the sum of all the thermally induced processes. A simple comparison of samples can provide practical and meaningful information even if the user has no real knowledge of the individual effects. These results are complemented by important data on the glass transition which are obtained in the same measurement.

Tips for databases

Customers often ask us about the most efficient method to manage their data. In UserCom 4 we gave a number of tips about organizing data in such a way as to facilitate a search later on (e.g. organization according to method group, project or task). In UserCom 8 we suggested how one can create meaningful filenames which are infact codes that indicate the content of the file.
Software Version V5.1x onwards allows you to choose between 5 different databases. The idea behind these databases is the following:

Each database should cover a certain period. We recommend, for example, a year, which would then give you one data base per year. Thanks to easy switching from one database to the other, you always have rapid access to the data from the last 5 years. Older data should be stored on an external device.

The optimum way of maintaining and using such a database is as follows:

- Weekly backup of data on an external device (e.g. DAT, ZIP or CD) or on a network server.
  Only the database actually selected is backed-up.
- Annual backup of the data on an external device.
- At the end of the year, the current database should be copied to the database of the new year (export it and import it into the new database on the hard disk). In this new database, all the data except that concerning methods, crucibles, gases, customers and the modules with their adjustment dates can be deleted. Customers who have the "Install Plus" software option can do this very simply with the following tip:

- always create methods under the "neutral" user name Mettler. If, later on, you want to delete these methods via the user, you should define a different "neutral" user name because the user name Mettler can not be deleted.
- Users should always work under their own user names.
  You therefore only have to delete all the users with their corresponding data in the database of the new year (delete all), and define new users and your new database is immediately ready for the new year.

Assuming your data has to be accessible for ten years, your database concept is similar to that described in the diagram below:

Stored on an external device									
DB2000	DB99	DB98	DB97	DB96	DB95	DB94	DB93	DB92	DB91
Stored on the hard disk									

Your data are then clearly structured and it is very easy to remove any data no longer required from the database.

Exhibitions, Conferences and Seminars - Veranstaltungen, Konferenzen und Seminare

Pittcon	March 13-16, 2000	New Orleans (USA)
ANALYTICA	11.-14. April, 2000	München (Deutschland)
INSTRURAMA	April 25-28 , 2000	Brussels (Belgium)
PLAST 2000	08-13 Maggio, 2000	Milano (Italy)
GEFTA-Tagung	17.-19. Mai, 2000	Dresden (Deutschland)
ACHEMA	22.-27.Mai, 2000	Frankfurt (Deutschland)
ASTM Symposium on Modulated Techniques	May 25-26, 2000	Toronto (Canada)
6th Laehnwitzseminar on Calorimetry	June 13-17, 2000	Kuehlungsborn (Germany)
ICTAC 2000	August 14-18, 2000	Copenhagen (Denmark)
NATAS	October 4-8, 2000	Orlando (USA)

TA Customer Courses and Seminars in Switzerland-Information and Course Registration: TA Kundenkurse und Seminare in der Schweiz-Auskunft und Anmeldung bei:

Helga Judex, Mettler-Toledo GmbH, Schwerzenbach,
Tel.: ++41-1 806 72 65, Fax: ++41-1 806 72 40, e-mail: helga.judex@mt.com

TMA (Deutsch)	13. März 2000	Greifensee	TMA/DMA (Deutsch)	11. September 2000	Greifensee
STARe SW Workshop Basic (D)	13. März 2000	Greifensee	STARe SW Workshop Basic (D)	11. September 2000	Greifensee
TGA (Deutsch)	14. März 2000	Greifensee	TGA (Deutsch)	12. September 2000	Greifensee
DSC Basic (Deutsch)	15. März 2000	Greifensee	DSC Basic (Deutsch)	13. September 2000	Greifensee
DSC Advanced (Deutsch)	16. März 2000	Greifensee	DSC Advanced (Deutsch)	14. September 2000	Greifensee
STARe SW Workshop Adv. (D)	17. März 2000	Greifensee	STARe SW Workshop Adv. (D)	15. September 2000	Greifensee
TMA (English)	March 20, 2000	Greifensee	TMA/DMA (English)	September 18, 2000	Greifensee
STARe SW Workshop Basic (E)	March 20, 2000	Greifensee	STARe SW Workshop Basic (E)	September 18, 2000	Greifensee
TGA (English)	March 21, 2000	Greifensee	TGA (English)	September 19, 2000	Greifensee
DSC Basic (English)	March 22, 2000	Greifensee	DSC Basic (English)	September 20, 2000	Greifensee
DSC Advanced (English)	March 23, 2000	Greifensee	DSC Advanced (English)	September 21, 2000	Greifensee
STARe SW Workshop Adv. (E)	March 24, 2000	Greifensee	STARe SW Workshop Adv. (E)	September 22, 2000	Greifensee

Workshop Tips und Hinweise für gute Messungen	20.11.99	Greifensee
Workshop Kurveninterpretation	21.11.99	Greifensee
Seminar Kopplungstechniken	22.11.99	Greifensee
Seminar Dynamisch Mechanische Analyse (DMA)	23.11.99	Greifensee

TA-Kundenkurse und Seminare (Deutschland)

Für nähere Informationen wenden Sie sich bitte an METTLER TOLEDO GmbH, Giessen: Frau Ina Wolf, Tel.: ++49-641 507 404.

DSC-Kundenkurs	29.2./1.3. 2000	Giessen/D
STARe SW Workshop	2.3. 2000	Giessen/D
DSC-Kundenkurs	7./8.11. 2000	Giessen/D
TG-Kundenkurs	9./10.11. 2000	Giessen/D
Thermogravimetrische Bodenanalyse – Grundlagen und Anwendungsmöglichkeiten eines neuen Analysenverfahrens	22.03.2000	Giessen/D
Fachseminar: Thermische Analyse an polymeren Werkstoffen in der Automobilindustrie	28.9. 2000	Giessen/D
DMA-Messtechnik – die Methode und ihre Anwendungen	29.9. 2000	Giessen/D

Cours et séminaires d'Analyse Thermique en France et en Belgique

France: Renseignements et inscriptions par Christine Fauvarque, Mettler-Toledo S.A., Viroflay,
Tél.: ++33-1 30 97 16 89, Fax: ++33-1 30 97 16 60.
Belgique: Renseignements et inscriptions par Pat Hoogeras, N.V. Mettler-Toledo S.A., Lot,
Tél.: ++32-2 334 02 09, Fax: ++32 2 334 02 10.

TMA (français)	2 Mai 2000	Viroflay (France)	Jour d'information	3 Mars 2000	Rouen (France)
TGA (français)	3 Mai 2000	Viroflay (France)	Jour d'information	21 Mars 2000	Paris (France)
DSC Basic (français)	4 Mai 2000	Viroflay (France)	Jour d'information	23 Mai 2000	Dijon (France)
DSC Advanced (français)	5 Mai 2000	Viroflay (France)	Jour d'information	20 Juin 2000	Grenoble (France)
TMA (français)	2 Octobre 2000	Viroflay (France)	Jour d'information	26 Septembre 2000	Mulhouse (France)
TGA (français)	3 Octobre 2000	Viroflay (France)	Jour d'information	6 Octobre 2000	Paris (France)
DSC Basic (français)	4 Octobre 2000	Viroflay (France)	Jour d'information	24 Octobre 2000	Paris (France)
DSC Advanced (français)	5 Octobre 2000	Viroflay (France)	Jour d'information	14 Octobre 2000	Montpellier (France)
Jour d'information	11 Janvier 2000	Nice (France)	Jour d'information	28 Novembre 2000	Poitiers (France)
Jour d'information	25 Janvier 2000	Clermont-Ferrand (F)	STARe user forum	4 Octobre 2000	Bruxelles (France)
Jour d'information	2 Février 2000	Metz (France)			

TA Customer Courses and Seminars in the Netherlands

For further information please contact: Hay Berden at Mettler-Toledo B.V., Tiel, Tel.: ++31 344 63 83 63.

Thermische Analyse seminar, basistraining	22.02.2000	Tiel/NL
Thermische Analyse seminar, gevorderde training	23.02.2000	Tiel/NL
STARe-Software seminar	24.02.2000	Tiel/NL

Corsi e Seminari di Analisi Termica per Clienti in Italia

Per ulteriori informazioni prego contattare: Simona Ferrari
Mettler-Toledo S.p.A., Novate Milanese, Tel.: ++39-2 333 321, Fax: ++39-2 356 2973.

Corsi per Clienti:	08-09 Marzo 2000	Novate Milanese		
	07-08 Giugno 2000	Novate Milanese		
	20-21 Settembre 2000	Novate Milanese		
Giornate di informazione:	03 Marzo 2000	Milano	29 Marzo 2000	Torino
	21 Marzo 2000	Napoli	30 Maggio 2000	Bologna
	22 Marzo 2000	Roma	31 Maggio 2000	Venezia
	23 Marzo 2000	Firenze		

TA Customer Courses and Seminars for Sweden and Nordic countries

For details of training courses ans seminars please contact:
Catharina Hasselgren at Mettler Toledo AB, Tel: ++46 8 702 50 24, Fax: ++46 8 642 45 62
E-mail: catharina.hasselgren@mt.com

TA Customer Courses and Seminars in USA and Canada

Basic Thermal Analysis Training based upon the STARe System version 6 is being offered April 21-22 and October 12-13 at our Columbus, Ohio Headquarters. Training will include lectures and hands-on workshops.
For information contact Jon Foreman at 1-800-638-8537 extension 4687 or by e-mail jon.foreman@mt.com

TA course	February 9 – 11, 2000	California	TA course	October 10 – 11, 2000	Columbus (OH)
TA course	June 21 – 22, 2000	Columbus (OH)	TA information day	February 8, 2000	California

TA Customer Courses and Seminars in UK

For details of training courses and seminars please contact:
Rod Bottom at Mettler-Toledo Ltd., Leicester, Tel.: ++44-116 234 50 25, Fax: ++44-116 234 50 25.

15 March 2000	Winchester	31 May 2000	Wakefield
22 March 2000	Glasgow	7 June 2000	Warrington
19 April 2000	Burton upon Trent	14 June 2000	Bristol
26 April 2000	Maidstone		

TA Customer training Course in South East Asia regional office, Kuala Lumpur

For information on dates please contact:

Malaysia:	Jackie Tan/Ann Owe	at ++ 603-7032773, fax: 603-7038773
Singapore:	Lim Li/Clive Choo	at ++ 65-7786779, fax: 65-7786639
Thailand:	Warangkana/Ajjima Sartra	at ++ 662-7196480, fax: 662-7196479
Or SEA regional office:	Soosay P.	at ++ 603-7041773, fax: 603-7031772

For further information regarding meetings, products or applications please contact your local METTLER TOLEDO representative.
Bei Fragen zu weiteren Tagungen, den Produkten oder Applikationen wenden Sie sich bitte an Ihre lokale METTLER TOLEDO Vertretung.
Internet: http:/www.mt.com

Redaktion

Mettler-Toledo GmbH, Analytical
Sonnenbergstrasse 74
CH-8603 Schwerzenbach, Schweiz

Dr. J. Schawe, Dr. R. Riesen, J. Widmann, Dr. M. Schubnell, U. Jörimann

e-mail: urs.joerimann@mt.com
Tel.: ++41 1 806 73 87, Fax: ++41 1 806 72 60

Layout und Produktion

Promotion & Dokumentation Schwerzenbach, G. Unterwegner
ME-51709991

Printed on 100% chlorine-free paper, for the sake of our environment.

METTLER TOLEDO